See: NIST SP861, W. L. Grosshandler, et al., Editors

7. CORROSION OF METALS

Richard E. Ricker, Mark R. Stoudt, James F. Dante, James L. Fink,
Carlos R. Beauchamp and Thomas P. Moffat
Materials Science and Engineering Laboratory

7.1 Introduction

Since a fire suppressant which is corrosive to either the materials used for storage and distribution of the agent or to aircraft materials after deployment would be undesirable, experiments were conducted to assess the relative corrosivity of the potential fire suppressants to different metallic alloys used on aircraft. These experiments were designed to evaluate the propensity of the different agents to cause failure by any of the possible corrosion failure modes during service or after deployment. In addition to these experiments, experiments were conducted to develop an electrochemical technique that would rapidly, and less expensively, evaluate the corrosivity of an agent and the influence of changes in composition, temperature and contaminant levels on the corrosivity of an agent.

Corrosion is usually defined as degradation of the properties of a material as a result of chemical reaction with the environment. Corrosion can be classified into different categories based on the material, environment, or the morphology of the corrosion damage. Based on the morphology of the damage, corrosion can be classified into eight different modes of attack:

1. General Corrosion - General corrosion is the result of chemical or electrochemical reactions which proceed over the entire exposed surface at about the same rate. General corrosion results in the metal becoming thinner and usually alters the appearance of the surface. General corrosion could result in failure through lowering the mechanical strength of components or by reducing wall thickness until leaking results.

2. Pitting Corrosion - Pitting corrosion is corrosion at a high rate in a small spot on the surface of a material. It commonly occurs at flaws in coatings applied to prevent corrosion of the underlying metal, but pitting corrosion also occurs in metals that resist corrosion through the formation of a native oxide, hydroxide or salt film ("passive" metals or alloys). To prevent corrosion, these films must be continuous and they must be able to reform rapidly by reaction between the material and the environment when the film cracks, ruptures or becomes damaged through any mechanical or chemical process. Apparently, halide ions either stimulate the breakdown of these films or inhibit their reformation (repassivation) as pitting is commonly observed in environments that contain ions of these elements. The time required to initiate pitting depends on temperature and the composition of the environment typically increasing in a logarithmic fashion as the halide ion concentration (activity) decreases. Once initiated, the corrosion rate at the bottom of a pit can be several orders of magnitude greater than that outside the pit and pitting could cause perforation of storage bottles, etc. or it could initiate cracks that propagate to failure by other mechanisms.

3. Crevice Corrosion - When a material is exposed to an environment, there are usually occluded regions, such as crevices, where the environment in this region does not freely mix with the bulk environment. The chemistry of the environment in these occluded regions can differ significantly from that of the bulk environment and this difference can result in corrosive attack. Crevice corrosion is frequently observed in passivated metals and alloys when they are exposed to environments that contain halide ions (especially chloride). Similar to pitting corrosion, a long incubation period may be required to initiate this attack, but once initiated, this attack can occur at rates that are orders of magnitude greater than rates outside the crevice. Crevice corrosion could result in failure through leaking of joints, mechanical failure of joints, freezing of joints, or it could lead to the initiation of cracks that propagate to failure through other mechanisms.

4. Intergranular Corrosion - Virtually all engineering alloys are fabricated by solidifying a melt composed of a mixture of elements. During this solidification process, crystals nucleate and grow together; forming the solid. As a result of this process, the chemical composition and the properties of the region between the crystals can differ significantly from those inside the crystals or grains. Alloy manufacturers have a variety of techniques that they employ to homogenize alloys and reduce this difference, but complete elimination of this difference is virtually impossible. As a result, certain alloy environment combinations can result in rapid corrosion of the region between the crystals. This is referred to as intergranular corrosion. When intergranular corrosion occurs, the surface of the material can appear unattacked, but the mechanical strength of the alloy can deteriorate slowly or rapidly until the materials break under any applied load or until individual grains begin to fall out and the material falls apart.

5. Environmentally Induced Fracture - When a material is exposed to a chemically reactive environment, the application of a mechanical stress to this material can result in the formation and propagation of a crack at stresses well below those required for cracking by purely mechanical processes in the absence of the corrosive environment. Exposure to aqueous solutions, organic solvents, liquid metals, solid metals, and gases have been found to cause failure in this manner. Depending on the environment and the type of loading, this type of failure has many different names such as stress corrosion cracking (SCC), chloride stress cracking, hydrogen embrittlement, liquid metal embrittlement, solid metal embrittlement, sulfide stress cracking, and corrosion fatigue, but they all consist of crack propagation induced by exposure to an environment. The environments that cause this type of failure are not always very aggressive and this mechanism of failure could cause sudden loss of agent or prevent the proper operation of valves.

6. Dealloying - Because different elements have different chemical activities, one element in an alloy may be selectively removed from the surface. This selective leaching of an alloying element can result in the surface becoming dealloyed and in some cases this dealloyed layer is not limited to the surface and it grows into the solid causing a serious loss of mechanical strength. In addition to lowering the strength of any component, dealloyed layers are porous and dealloying could cause loss of agent from a storage container.

7. Galvanic Corrosion - Because different elements have different chemical activities, different alloys with different chemical compositions will have different chemical and

electrochemical properties in the same environment. Joining of dissimilar metals in a manner such that an electrical circuit is completed through the joint and the environment will result in increasing the rate of corrosion of the more active metal and reducing the rate of corrosion of the more noble metal. The extent of the change depends on a variety of factors including the ratio of the areas of each alloy exposed to the environment, the potential difference between the alloys, the electrical resistivity of the joint, and the conductivity of the environment. In the case of metals and alloys exposed to fire suppressants, the conductivity of these suppressants is usually extremely low (unless they become contaminated with impurities) and this should minimize the damage that galvanic coupling of dissimilar alloys can cause.

8. Erosion Corrosion - Mixing or stirring of a solution can accelerate the rate of corrosion either by simply increasing the rate of transport to the surface or by mechanically damaging or removing surface films that may protect the underlying metal from attack. An increase in the rate of corrosion as a result of relative motion of the environment is termed "erosion corrosion." In general, the relative motion of the agents in the storage and distribution systems will be quite low; except during deployment, where erosion corrosion may occur in the nozzles.

Of these eight corrosion failure modes, six are of potential concern for the storage, distribution, and post deployment corrosivity of fire suppressant agents on aircraft: general corrosion, pitting corrosion, crevice corrosion, intergranular corrosion, environmental induced fracture and dealloying. Erosion corrosion may be a concern for nozzles but, the duration of the flow through the nozzle is very short and damage by this mechanisms should be noted in the fire suppressant efficiency tests if it occurs. Galvanic coupling may influence corrosion damage accumulation, but due to the relatively low conductivity of these agents, galvanic effects should be at a minimum. As a result, experiments were designed to evaluate the propensity of the different agents to cause failure by these six corrosion failure modes.

On board aircraft, metallic materials will be exposed to fire suppressant agents during storage (storage containers, valves etc.), deployment (distribution tubes, nozzles, etc.) and post-deployment (structural and engine components exposed to residuals and combustion products) but, the exposures during deployment are very short and should not be of concern. Of greatest concern for the safe operation of aircraft is the possibility that the fire suppressant might cause attack of the storage container resulting in loss of agent or preventing the proper operation of the release valve. These storage containers hold the agent for up to five years at high pressures (≈ 5.8 MPa) and temperatures as high as 150 °C. Very little is known about the corrosion of metals in these environments and there is virtually no information in the literature on the corrosivity of most of these agents to the metals used for aircraft storage containers. As a result, corrosion experiments that emulate the suppressant storage conditions were determined to be a necessary part of the evaluation of new fire suppressant agents.

A second concern for the safe operation of aircraft, is the potential for significant corrosion damage to the structural metals of the aircraft and aircraft components by residual suppressant or by suppressant combustion products. Of particular concern would be the formation of halide acids or salts as a result of the combustion of the agent during fire suppression. For suppressants that are not a gas at normal temperatures and pressures, residual suppressant left on the surface of metals after suppressant deployment could result in corrosion damage before the agent is cleaned off the surface (30 days maximum exposure). As a result of this concern, experiments were designed to evaluate the potential for corrosion damage to metals by suppressant residual and combustion products.

7.2 Experimental

There were two main objectives of this initial phase of the study: 1) to rank the corrosivity of the alternative fire suppressants with respect to storage vessel materials and 2) to rank the corrosion resistance of the storage vessel materials when exposed to alternative fire suppressants. This allows the elimination of the most corrosive fire suppressants and the least corrosion resistant storage vessel material. To achieve these objectives, experiments were designed to evaluate the propensity of the different agents to cause failure by the possible corrosion failure modes during service or post-deployment. In addition to these experiments, experiments were also conducted to develop an electrochemical technique that would rapidly, and less expensively, evaluate the corrosivity of an agent and the influence of changes in composition, temperature and contaminant levels on the corrosivity of an agent.

7.2.1 Aircraft Storage System Corrosion. Experiments were designed and conducted to evaluate the corrosivity of the different potential fire suppressants during normal service in aircraft storage containers. Since no electrochemical techniques have been developed for the rapid evaluation of the corrosivity of low conductivity media such as fire suppressants, these experiments had to consist of exposures that emulate the conditions under which corrosion is expected to occur followed by careful examination and evaluation of the resulting corrosion damage. To evaluate the potential for failure of the aircraft storage containers by the six potential corrosion failure modes during normal service, three different types of exposures tests were conducted to evaluate the potential for failure of the aircraft storage containers by the six possible corrosion failure modes expected during normal service. Exposure tests were conducted to determine the changes in mass during the exposures which would, in turn, assess the rate of formation of corrosion scales or the rate of removal of metallic species by corrosion. Also, visual and optical microscope examination of these samples after exposure allowed for the evaluation of the occurrence of pitting, intergranular corrosion and dealloying. Using the mass change and the exposure time data, the average mass change was estimated allowing for a comparison between the agents. The weld/crevice coupon exposures were conducted to allow for the evaluation of localized corrosion failure modes such as crevice corrosion, weld zone attack, and intergranular attack in the heat affected zone. The environmental induced fracture resistance of the alloys in the agents was evaluated by conducting exposure tests on cylindrical samples of the alloys that are loaded in tension by slowly increasing the strain on the sample until failure occurs by either normal mechanical means or by an environmentally assisted or induced means (the slow strain rate tensile test). By comparing the strain or load required to cause failure in an inert environment to that required to cause failure in the agents, the propensity of each agent to cause environmentally induced fracture in each alloy can be evaluated.

7.2.1.1 Materials. The following materials were chosen for this study: 304 stainless steel, 13-8 Mo stainless steel, AM 355 stainless steel, stainless steel alloy 21-6-9 (Nitronic 40), 4130 alloy steel, Inconel alloy 625, CDA-172 copper/beryllium alloy and 6061-T6 aluminum alloy. (The compositions of these alloys are given in Table 1.) These alloys were selected for these experiments based on discussions with the Air Force on the materials typically used for aircraft storage containers and distribution system components.

7.2.1.2 Mass Change (Smooth Coupon) Exposure Experiments. The samples used for the mass change experiments were flat smooth surface coupons of the geometry shown in Figure 1(a).

Table 1. Composition of the alloys in weight percent

Element	Nit 40	Al 6061	In 625	304 SS	CDA 172	13-8 Steel	AM 355	AISI 4130
Ni	7.1	- -	61.39	8.26	0.06	8.4	4.23	0.08
Cr	19.75	0.04	21.71	18.11	0.01	12.65	15.28	0.98
Mn	9.4	0.15	0.08	1.41	- -	0.02	0.8	0.51
Mg	- -	1	- -	- -	- -	- -	- -	- -
Si	0.5	0.4	0.09	0.49	0.08	0.04	0.16	0.23
Mo	- -	- -	8.82	0.17	- -	2.18	2.6	0.16
Nb	- -	- -	3.41	- -	- -	- -	- -	- -
N	0.29	- -	- -	0.03	- -	0	0.12	- -
C	0.02	- -	0.02	0.06	- -	0.03	0.12	0.32
Be	- -	- -	- -	- -	1.9	- -	- -	- -
Co	- -	- -	- -	0.11	0.2	- -	- -	- -
Zn	- -	0.25	- -	- -	- -	- -	- -	- -
Cu	- -	0.15	- -	- -	97.9	- -	- -	- -
Fe	bal	0.7	3.97	bal	0.06	bal	bal	bal
Al	- -	bal	0.23	- -	0.04	1.11	- -	0.04
g/cm^3[a]	7.83	2.70	8.44	7.94	8.23	7.76	7.91	7.85
kg/m^3	7,830	2,700	8,440	7,940	8,230	7,760	7,910	7,850

[a]Nominal Density

After machining, the surfaces were glass bead blasted to remove any remaining surface oxides or scale and to provide a consistent smooth surface finish (120 grit nominal). Additional preparation prior to the start of these tests consisted of cleaning and three initial weight measurements for each individual sample. Each sample was ultrasonically cleaned, first in acetone and then in alcohol, dried with warm air and immediately weighed. Three separate weighings were taken at approximately 30 second intervals and averaged. This average value was then referred to as the initial weight of the coupon. The balance used for these weight measurements was self calibrating on start-up to maintain an accuracy to within $\pm 10 \times 10^{-6}$ g with a reproducibility of no less than $\pm 1.51 \times 10^{-8}$ g. Representative photographs of the surface of each alloy were also taken prior to the start of testing.

At the start of each exposure test, three coupons of each of the eight alloys were mounted on a polytetraflouroethylene (PTFE) rod with PTFE spacers between the samples as shown in Figure 2. This was done 1) to separate and 2) to isolate the samples electrically; thus eliminating galvanic coupling effects. Three samples of each alloy type were tested and PTFE shields were placed between the different alloys sets to protect the samples from contact with any corrosion products that may form. The samples were next placed in a custom designed PTFE liner and charged into a two

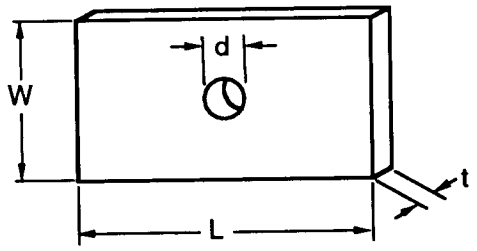

W= 25.4 mm (1.0 in)
L= 50.8 mm (2.0 in)
t= 1.6 mm (0.0625 in)
d= 6.7 mm (0.265 in)

(a) General corrosion coupon design (ASTM G-01).

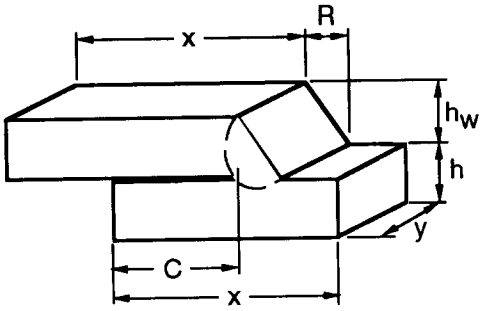

x = 50.8 mm (2.0 in)
y = 50.8 mm (2.0 in)
R = 4.75 mm (0.1875 in)
C = 31.75 mm (1.25 in)
h = 3.2 mm (0.125 in)
h_W = 3.2 mm (0.125 in)

(b) Weld/crevice corrosion coupon design.

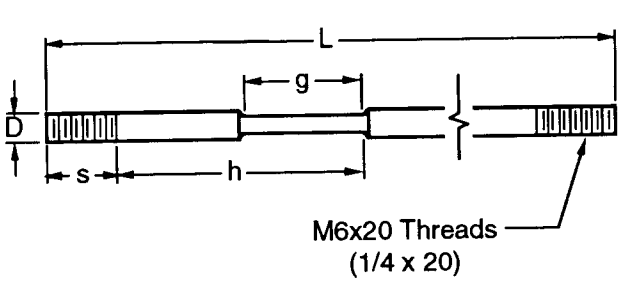

D = 19 mm (0.25 in)
L = 178 mm (7 in)
g = 25.4 mm (1 in)
h = 57 mm (2.25 in)
s = 19 mm (0.75 in)

(c) Slow strain rate tensile sample design (ASTM E-8, G-49).

Figure 1. Design of samples used in immersion and slow strain rate tensile tests.

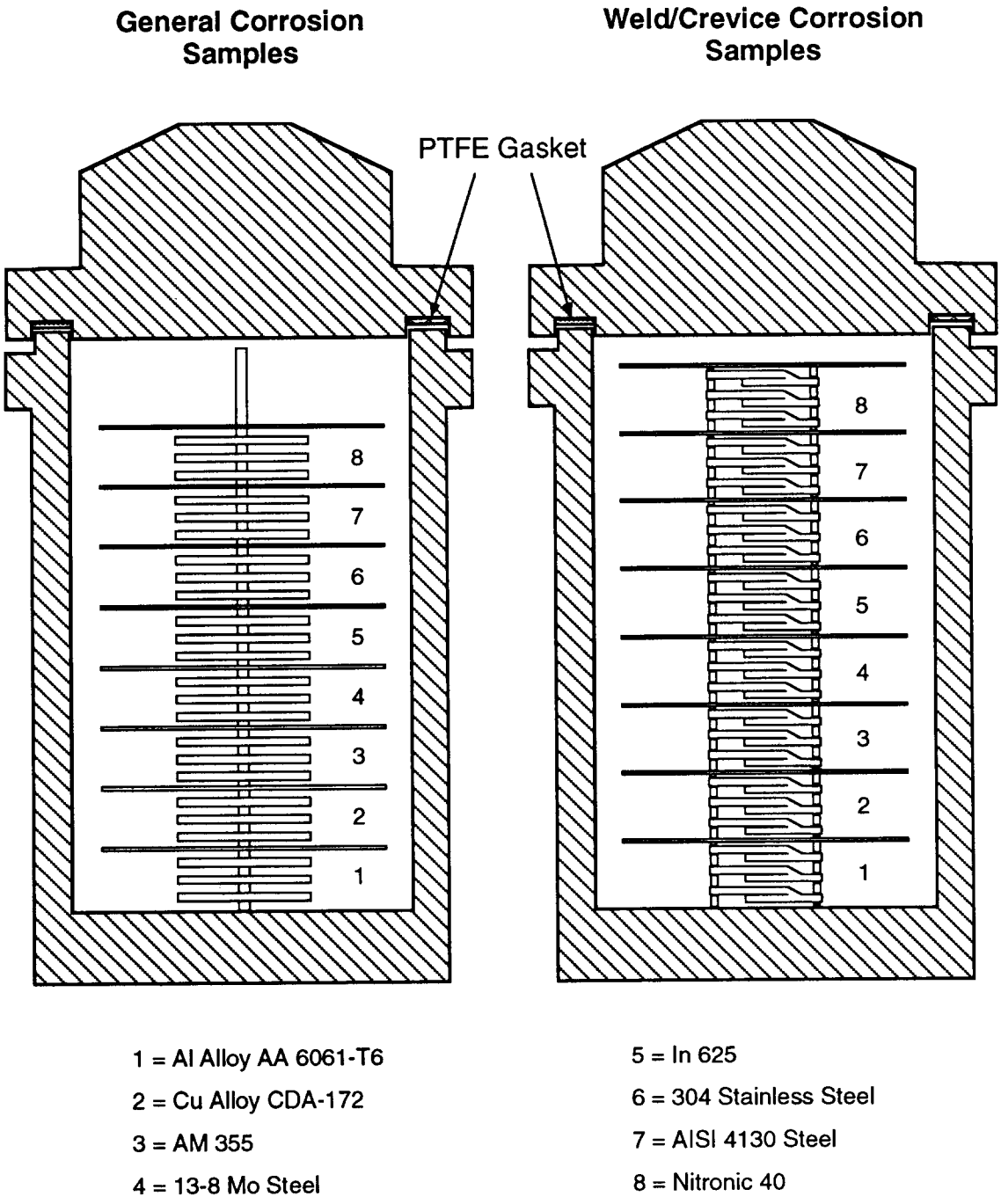

Figure 2. Immersion testing chamber used for general corrosion coupon tests and weld/crevice corrosion coupon tests.

liter pressure vessel for testing. The vessel was then attached to a mechanical vacuum pump and evacuated for a minimum of 30 minutes.

The mass of agent required to produce a pressure of approximately 5.86 MPa at 150 °C was determined by using the mass balance shown in Equation 1:

$$M_T = \rho_1 V_1 + \rho_g V_g \quad (1)$$

where M_T is the total mass of the system, ρ_l is the density of the liquid agent at 20 °C, V_l is the volume of the liquid agent at 20 °C, ρ_g is the density of the vapor phase at 20 °C, and V_g is the volume of the vapor at 20 °C. A computer program based on Equation 1, the available thermodynamic data, and the ideal gas law was developed to calculate the required mass. To facilitate charging of the agents, the test vessels were chilled in a bath of either ice and water, or dry ice and alcohol, depending on the temperature necessary to maintain the liquid phase. The vessels were then placed on a balance that allowed weighing of the entire vessel and determination of the mass of the agent added continuously during filling. Upon completion of the charging step, the vessels were placed in proportionally controlled, calrod-type heaters that kept the temperature constant at 150 ± 1 °C for the 25 day exposure period.

At the conclusion of the testing period, the heaters were turned off and the vessels were allowed to cool naturally to ambient temperature. After the agent was released, the coupons were extracted and immediately re-weighed using the same procedure that was used for the initial weight measurements. The average of those three measurements was then referred to as the final weight of the coupon. Representative photographs of the surfaces were again taken and compared to those of the initial condition.

7.2.1.3 Localized Corrosion (Weld/Crevice Coupon) Exposure Experiments. The samples used for these experiments were designed to provide specific information about changes in the nature of the corrosion in a crevice and in a weld heat affected zone. The geometry of these is shown in Figure 1(b). The testing procedure used for these experiments was identical to the procedure used for the smooth coupon mass change experiments except that the samples were not weighed before and after the exposures.

At the conclusion of the 25 day test period, the samples were removed from the test chambers and the samples were split along the fusion boundary using a water cooled slitting saw. The internal surfaces of the crevice were then analyzed by eye and in an optical microscope. The resulting appearance within the crevice region of the three samples for each agent/alloy combination was then given a numerical rating based on the appearance of the corrosion damage within the crevice region. In addition, the relative performance of each alloy in a given agent was determined by placing all of the samples tested in that agent on a table and making direct (optical) comparisons. Then, the relative corrosivity of the different agents for a given alloy was determined by placing all of the samples of that type of alloy on a table and making direct (optical) comparisons between the damage that resulted in each agent.

7.2.1.4 Environmental Induced Fracture (Slow Strain Rate Tensile Tests). The stress corrosion cracking susceptibilities of the eight alloys in the replacement candidates were evaluated using the slow strain rate (SSR) tensile test technique. This technique was selected because it generates mechanical properties data that reveals any interactions that may have occurred between that alloy and the testing environment within a relatively short time frame.

All of the samples used for these experiments were machined with the tensile axis parallel to the rolling direction of the plate stock (Figure 1(c)) and tested in the "as received" condition. The sample preparation consisted of measurement followed by degreasing in acetone and alcohol. The vessels used for these experiments, Figure 3, were 250 ml volume autoclaves with a similar design to those used for the exposure testing, except that these vessels were modified so that load could be applied to the tensile specimen *in situ* under constantly maintained environmental conditions (5.86 MPa at 150±1 °C). The test vessels were evacuated and charged with agent in the same manner as the exposure test vessels, but due to the number of mechanical tests required per agent, and the reduced capacity of the test vessels, the appropriate mass was based solely on the ideal gas law. This approach was selected over the mass balance because it produced a slightly lower final pressure and the number of moles of the agent was held constant for each test; regardless of the agent used.

The mechanical tests were conducted using a computer controlled slow strain rate testing system which operated at a constant crosshead speed of 0.0254 μm/sec. The computer was configured to sample and record the applied load, the crosshead displacement and the elapsed time at 90 second intervals. After failure, the agent was released, the vessels were allowed to cool to ambient temperature, and the samples were removed from the vessel and stored in a desiccator until analyzed.

The fracture surfaces were cut from the broken SSR samples for analysis. The influence of the agents on the ductility of the alloys was determined from reduction in area (RA) measurements performed on the fracture surfaces with a optical measuring microscope with a $\pm$ 0.5×10^{-6} m resolution. Scanning electron microscopy was performed on selected samples to allow evaluation of the mechanism of crack propagation based on the fracture morphology. The results of these experiments were used to formulate a ranking of the potential for failure by stress corrosion cracking for each of the alloys in a replacement candidate.

7.2.2 Post Deployment Experiments. When a fire suppressant is applied to a fire, the metals in the aircraft engine nacelle or dry bays may become covered with deposits of the fire suppressant or fire suppressant combustion products. As a result, an evaluation of the relative corrosivity of the expected combustion product layers was included in this investigation.

7.2.2.1 Materials and Sample Preparation. The alloys used for these experiments were the same as those used for the aircraft storage and distribution system experiments. These alloys were used because samples were readily available and because this matrix included representative alloys of the different types that might be exposed to fire suppressant combustion products. The samples used were identical to those given in Figure 1(a) except that these samples did not contain the hole in the center. As before, the samples were glass bead blasted to the equivalent of a 120 grit finish. The samples were cleaned in acetone in an ultrasonic cleaner and then treated with acid solutions in an ultrasonic cleaner to remove existing corrosion products and surface films. The acid solutions were rinsed off of the metal surfaces using distilled water. Following is a list of the acid mixtures used for surface cleaning or pretreatment:

- **6061-T6**. The surface was treated by exposing it to concentrated HNO_3 for three minute intervals until the mass loss for this exposure time became constant.

- **CDA-172**. The surface was treated by exposing it to 250 ml of a solution made by adding 25 ml of H_2SO_4 to double distilled water for three minute intervals until the mass loss for this exposure became constant.

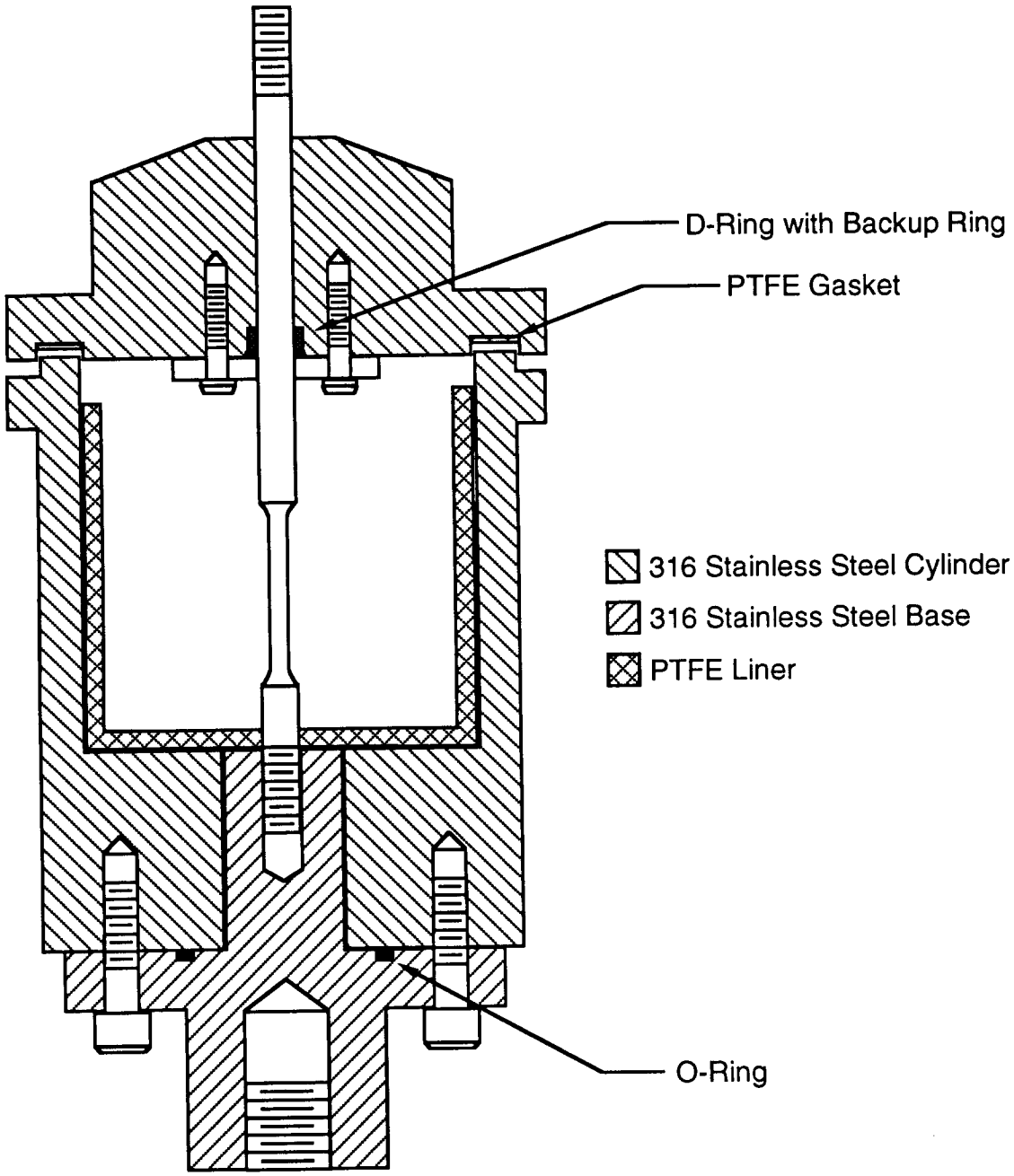

Figure 3. Slow strain rate tensile test chamber.

- **IN 625**. The surface was treated by exposing it to 250 ml of a solution made by adding 37.5 ml of HCl to double distilled water for three minute intervals until the mass loss for this exposure became constant.

- **AISI 4130, AM 355 and 13-8 Mo Steel**. A solution was prepared by adding 80 ml of a 35 weight % solution of 2 butyne 1,4 diol to 60 ml of HCl and then adding double distilled water to make one liter of solution. The AM355 and 13-8 Mo surfaces were exposed to this mixture for three minute intervals until the mass loss for this exposure became constant. The 4130 surface was exposed to this mixture for one minute intervals until the mass loss for this exposure became constant. The 4130 steel became tarnished by the water rinse used to clean the surface.

- **Nitronic 40 and 304 Stainless Steel**. One liter of solution was prepared by adding 100 ml of HNO_3 to 20 ml to double distilled water. The samples were exposed to this mixture for five minute intervals until the mass loss for this exposure became constant.

7.2.2.2 Combustion Product Surface Layer Emulation. The fire suppressant candidates can be classified into two categories: those that contain fluorine and/or other halides and those that contain sodium bicarbonate. Fire suppressants that contain halides, of which fluorine is usually the worst, will produce halide ions during combustion that will deposit on metallic surfaces and form halide acids when they react with water. Sodium bicarbonate ($NaHCO_3$) will decompose on heating to form sodium carbonate (Na_2CO_3), and on combustion to form sodium hydroxide (NaOH). As a result, there are essentially three different combustion product surface films of interest: (1) fluoride ions, (2) $NaHCO_3/Na_2CO_3$ and (3) NaOH.

To produce a surface film rich in fluoride ions, the surface of the samples were first sprayed with ASTM artificial seawater then sprinkled with sodium fluoride (NaF) powder while the surface was still wet. While the films produced by combustion will be much more complex than this simple analog, this surface film should contain the most critical corrosive species that can be expected following deployment: water, chloride and fluoride. The ASTM seawater step was included to simulate the conditions in a marine atmosphere, which should be the worst case situation, as well as to provide water for reaction with the sodium fluoride. To simulate the sodium bicarbonate and sodium carbonate ($NaHCO_3/Na_2CO_3$) surface film, the samples were sprayed with ASTM artificial seawater and sprinkled with a 50/50 mixture of sodium bicarbonate/sodium carbonate. The 50/50 mixture was created by heating 100 g of sodium bicarbonate + 1.5 weight % SiO_2 overnight at 150 °C to form sodium carbonate and then mixing this with another 100 g of sodium bicarbonate + 1.5 weight % SiO_2. To simulate the NaOH rich surface film that may result from the deposition of $NaHCO_3$ combustion products, the samples were sprayed with ASTM artificial seawater and then sprayed with a 0.1 M solution of NaOH. The samples were placed into their exposure chambers immediately following these surface treatments.

7.2.2.3 Exposure Environment. After deployment of a fire suppressant, a layer of combustion products may remain on the exposed surfaces for up to one month before the surfaces are cleaned to remove the surface film. During this time, the environment which will cause corrosion will be the ambient air environment and the hydration of the surface film that may result from absorption of water from the ambient environment (corrosion in condensate droplets as a result of thermal cycling was not included in this study). As a result, the exposures were conducted in three different glass desiccators each with the a different fixed relative humidity (RH). To keep the relative humidity constant, the desiccant in each of the desiccators was replaced with a saturated salt solution which has

a different equilibrium water vapor partial pressure or relative humidity. For a low relative humidity exposure, a saturated solution of potassium acetate ($KC_2H_3O_2$) was included in the desiccator for which the equilibrium relative humidity is 20%. For a moderate relative humidity environment, a saturated sodium dichromate dihydrate ($Na_2Cr_2O_7 \cdot 2H_2O$) solution was used in the desiccator for which the equilibrium relative humidity is 52%. And for a high relative humidity, a saturated solution of sodium sulfate decahydrate ($Na_2SO_4 \cdot 10H_2O$) for which the equilibrium relative humidity is 93% was used.

7.2.2.4 Testing Procedure. The samples of the different alloys were exposed under nine different conditions: three different pretreatments and three different humidities. The samples were weighed between the cleaning and the surface pre-treatment steps. After the application of the ASTM artificial seawater, the samples were weighed again in order to determine the mass present on the surface. Then, after the NaF, 50/50 $NaHCO_3$/Na2CO3 mixture, or the NaOH was applied, the samples were weighed again. Then, the specimens were exposed for 30 days with one of each alloy and pretreatment in each humidity. Following the exposure, the coupons were weighed, then rinsed in double distilled water, dried and reweighed. Finally, the corrosion product films were chemically removed by using the same cleaning procedure used during the sample preparation and the samples were weighed again to determine the total mass loss due to corrosion.

7.2.3 Development of an Electrochemical Measurement Technique. Electrochemical techniques can be used to measure the interfacial properties directly associated with the rate of corrosion. These measurements allow for a relatively fast determination of the corrosion resistance of a metal or alloy in solution as compared to the time required for acquisition of similar data from exposure tests in the same environment. The development of such a technique would provide a more thorough assessment of the corrosion rates of the storage vessel materials in the alternative fire suppressants.

Figure 4 is a schematic representation of the most simple equivalent electrical circuit that can be used to describe the processes that occur in an electrochemical cell. In this figure, R_s represents the resistance between the sample and the measurement point that arises due to the resistivity of the electrolyte, C_{dl} is the capacitance of the sample electrode solution interface and R_{ct} is the charge transfer resistance that arises from the kinetics of the electrochemical reactions occurring at the electrode surface (*e.g.*, corrosion). If R_s is high, as in the case of the extremely high resistivity associated with fire suppressants, significant error or artifacts in the measured interfacial properties can be expected. Therefore, a technique must be developed to either 1) reduce the solution resistivity (without compromising the relative order of corrosivity of the agents) or 2) allow for the correction of the solution resistivity and eliminate the observed artifacts. Experimentally, the best approach for obtaining useful data is done by applying a low amplitude sine wave to the sample and measuring the cell impedance as the frequency of the sine wave is varied. By examining Figure 4, it can be seen that for a low frequency sine wave the impedance of this circuit becomes R_s+R_{ct}, while for a high frequency signal the impedance of the circuit becomes just R_s. This technique is known as ac impedance or electrochemical impedance spectroscopy (EIS).

For EIS, one normally uses a potentiostat and three electrode cell, Figure 5. The sample, a reference electrode and a counter electrode make up the three electrodes in this system. This allows for the measurement of the potential of the sample with respect to a reference electrode with a fixed and well known potential on the hydrogen electrode (thermodynamic) scale while applying current with a counter electrode whose potential can vary with current without creating measurement errors. However, as the resistivity of the media increases, problems arise due to the appearance of artifacts which result in considerable measurement errors. Investigators have shown that a two electrode system is more suited for EIS measurements in high resistivity media than a three electrode system

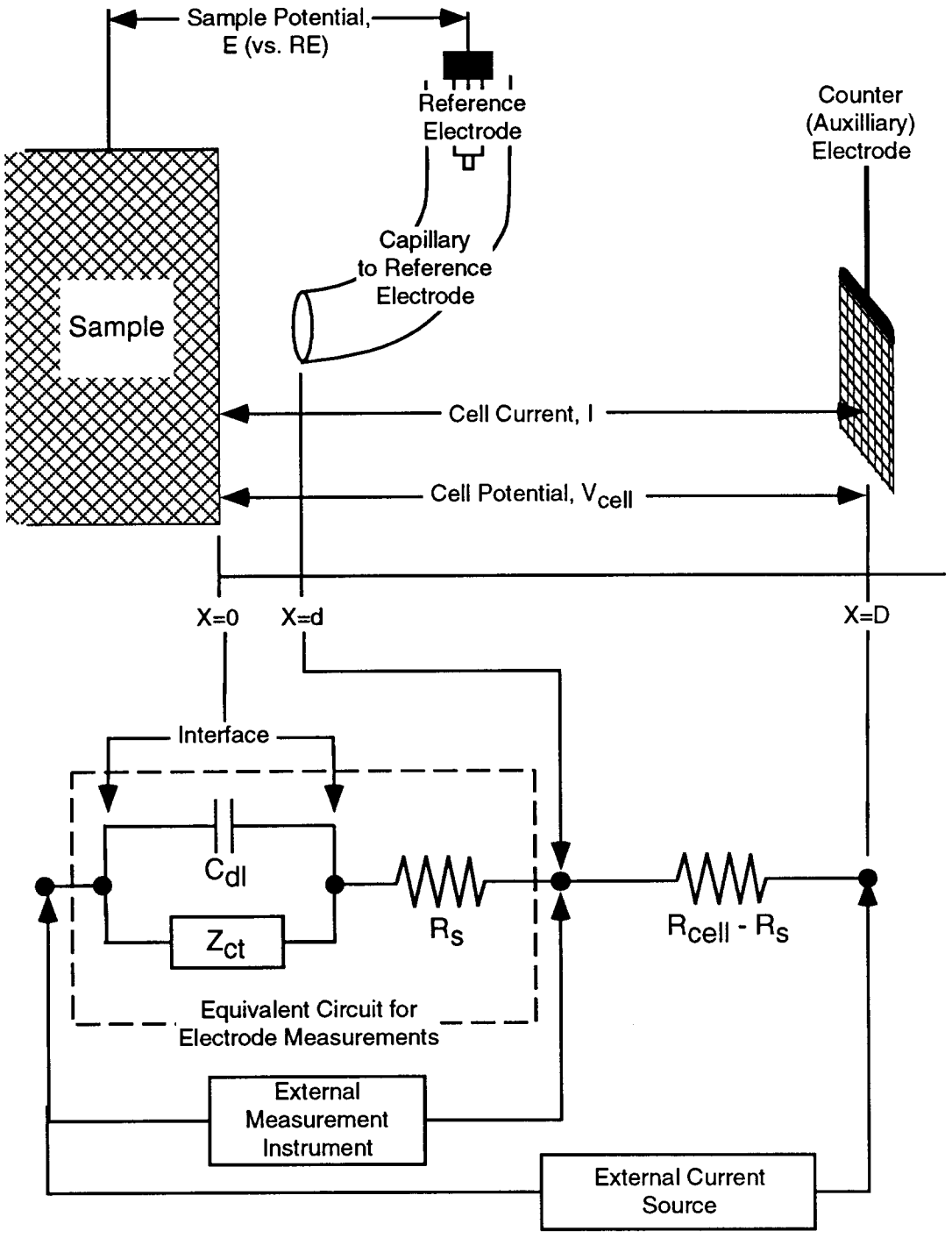

Figure 4. Simple equivalent circuit for an electrochemical interface.

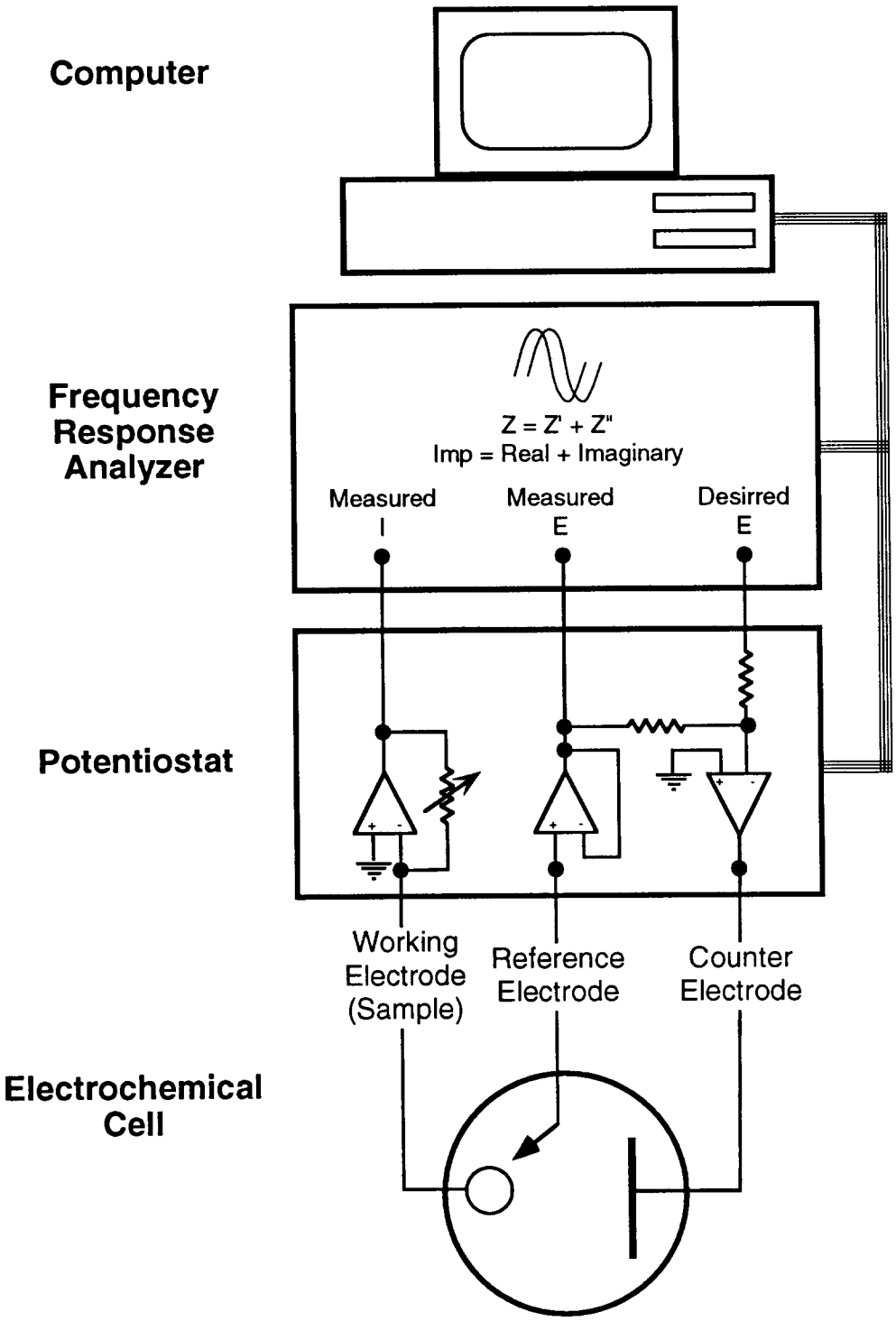

Figure 5. Simple diagram of a three electrode cell used for electrode impedance measurements.

(Halsal, 1992, and DeSouza, 1986). As a result, a two electrode cell capable of placing two relatively large area samples in close proximity and conducting EIS measurements at different temperatures and pressures was designed and fabricated. This cell design is shown schematically in Figure 6 and consists essentially of a autoclave similar to that used for the exposure tests modified by the addition of electrical feed troughs in the head along with a micrometer for adjusting the distance between the samples. Inside the chamber, two identical disk samples are held in place by PTFE holders one of which is moved by the micrometer. To evaluate the functionality of this chamber, measurements were made on samples in an environment similar to that used by the previous investigators (Halsal, 1992, and DeSouza, 1986).

7.2.3.1 Materials. Disk shaped samples 38 mm in diameter and 12.7 mm thick were machined out of 304 stainless steel and polished to a 0.05 μm finish. Before placing the samples into the cell, they were rinsed with reagent anhydrous ethyl alcohol. Anhydrous ethyl alcohol with approximately 0.005 % water and a conductivity on the order of 10^{-6} ohms^{-1} cm^{-1} was used initially for the testing environment because this is similar to the environment used by the previous investigators. It should be remembered that the conductivity of the halon alternatives is orders of magnitude lower than this value. However, results of tests performed in ethyl alcohol should reveal the effectiveness of the cell in measuring electrochemical parameters in low conductivity media. The addition of nonaggressive charge carriers to the fire suppressants may increase their conductivity up to or above this level.

7.2.3.2 Procedure. After the cell was assembled, ethyl alcohol was introduced. The initial separation distance of the electrodes was measured. The impedance of this cell at different frequencies from 65,000 Hz to 0.1 Hz was determine with a 10 mV amplitude signal. From this data, the solution resistance was determined. The separation of the electrodes was increased by 1 mm and another scan was taken. This procedure was repeated until the electrodes were 4 mm from there original position. The electrodes were then reset to their original position and the entire procedure was repeated.

7.3 Results

7.3.1 Aircraft Storage and Distribution System Corrosion.

7.3.1.1 Mass Change (Smooth Sample) Exposure Experiments. The mean mass changes observed for three samples of each of the alloys on exposure to each of the agents for 25 days at 150 °C are given in Table 2, the standard deviation determined for these measurements are given in Table 3 and the original measurements are given in Appendix A. On examination of these tables, it can be seen that all of the mass changes are relatively small and most are mass increases (positive values in Table 2). The mass change rate was estimated from these mass change measurements from the relationship

$$R = \frac{\Delta M}{At} \tag{2}$$

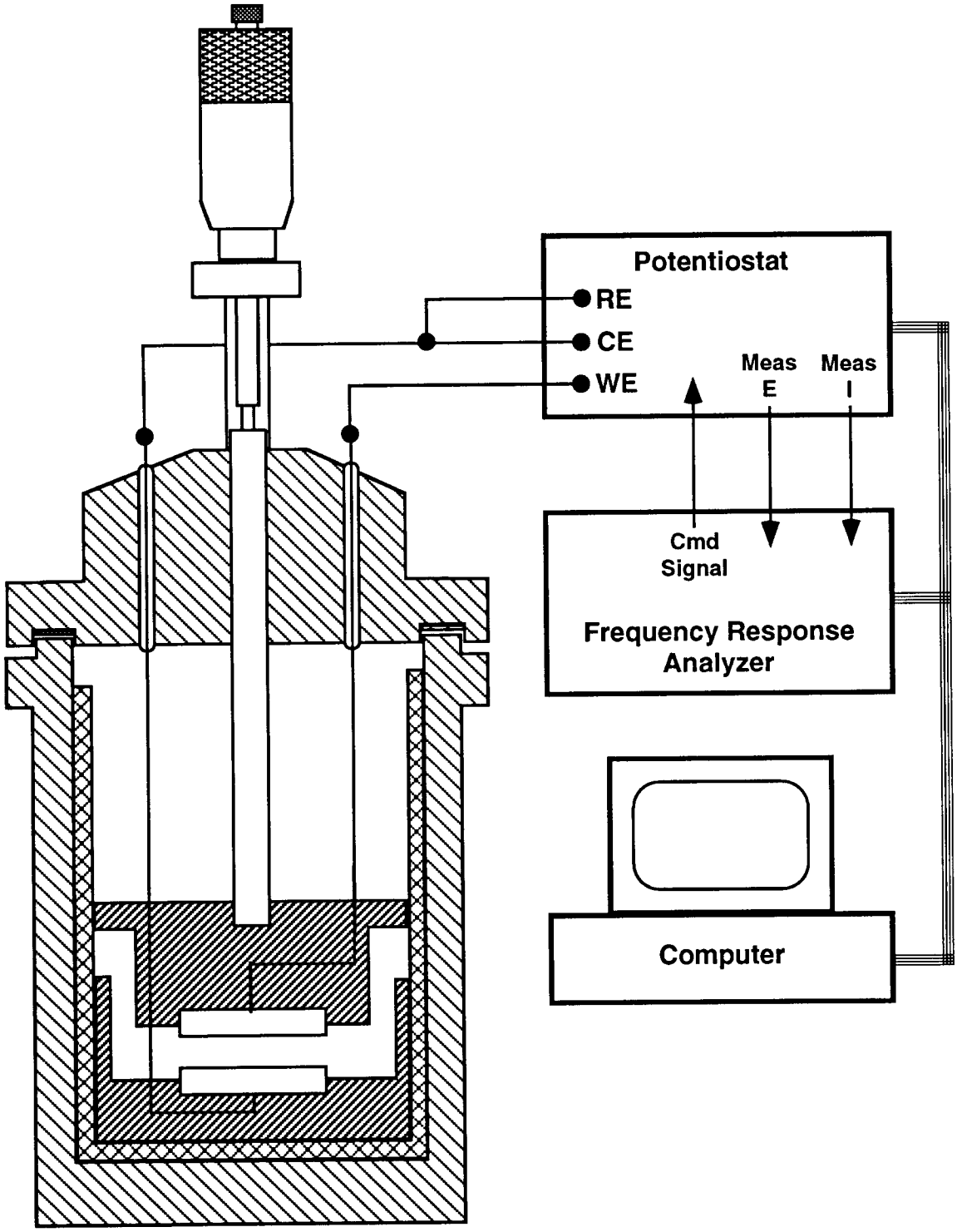

Figure 6. Electrochemical cell for two electrode impedance measurements in low conductivity electrolytes at elevated temperatures and pressures.

Table 2. Mean Mass Change for the three samples of Each Alloy tested in Each Agent After 25 Day Immersion at 150 °C [mg]

Environment	Nit 40	Al 6061	In 625	304 SS	CDA 172	13-8 Steel	AM 355	AISI 4130	Agent Avg.	Std. Dev.
HCFC-22	0.176	0.458	-0.329	0.168	3.064	-0.033	-0.087	2.847	0.783	1.362
HCFC-124	0.092	0.219	-0.267	-0.037	1.474	-0.086	-0.206	0.319	0.189	0.557
FC-31-10	0.247	0.533	-0.037	0.583	2.663	0.357	0.219	1.102	0.708	0.858
HFC-227	0.009	0.128	-0.056	0.141	1.973	0.069	0.007	0.297	0.321	0.676
HFC-125	-0.011	0.199	0.031	0.136	0.890	0.151	0.029	0.673	0.262	0.333
FC-116	0.006	0.240	0.026	0.147	1.509	0.210	0.139	0.403	0.335	0.491
HFC-134a	0.013	0.131	-0.103	0.069	0.229	0.088	-0.014	0.262	0.084	0.122
HFC-236	0.024	2.479	-0.063	0.078	0.866	0.107	0.007	0.343	0.480	0.861
FC-C318	0.008	1.183	0.018	0.199	0.431	0.169	0.006	0.310	0.290	0.392
FC-218	0.153	0.373	0.051	0.090	0.768	0.279	0.150	0.381	0.281	0.232
HFC-32/125	0.300	0.587	0.146	0.241	2.263	0.492	0.311	0.227	1.960	3.851
NaHCO3	0.396	1.038	0.079	0.262	2.182	0.800	0.259	0.890	0.738	0.677
Alloy Avg.	0.118	0.631	-0.042	0.173	1.526	0.217	0.068	1.597		
Std. Dev.	0.137	0.675	0.138	0.152	0.911	0.243	0.150	3.152		

Positive Values = Scaling
Negative Values = Mass Loss

where ΔM is the mass change, A is the total exposed area of the sample and t is the exposure time in days and are given in Table 4. This relationship estimates the average mass change rate over the exposure period and assumes that the mass change rate was essentially constant over the entire exposure period.

The magnitudes of these mass changes (Table 4) are small but, they are, for the most part, larger than that required to be statistically significant for the measurement equipment and measurement techniques employed. Since each sample was weighed three times before and after each exposure, the standard deviation for the mass measurement process can be estimated and it was found to be less than 1.4×10^{-5} g. If one conducts a t-test for the significance of the change in mass based on this estimated standard deviation, one will find t values that indicate significant mass change at the 99% confidence level in all but 20 of the 96 agent/alloy combinations. However, when the mass change measurements over the three samples of each alloy tested in each agent are averaged, a larger standard deviation is determined because this standard deviation includes scatter from the natural corrosion processes and sample handling during preparation and removal from the exposure chamber in addition to the normal measurement scatter. In Table 5, a minimum and maximum mass change rate at the 90% confidence level is given for each alloy/agent combination. The values in this table were determined from the standard deviation estimated from the three samples of each alloy tested in each agent and estimated standard deviations for the surface area and exposure time using standard

Table 3. Standard Deviation of mass change measurements for the three samples of each alloy tested in each environment (mg)

Environment	Nit 40	Al 6061	In 625	304 SS	CDA 172	13-8 Steel	AM 355	AISI 4130	Agent Avg.
HCFC-22	0.079	0.113	0.088	0.057	0.331	0.043	0.050	1.280	0.255
HCFC-124	0.045	0.091	0.048	0.040	0.294	0.072	0.103	0.099	0.099
FC-31-10	0.040	0.079	0.028	0.035	0.107	0.070	0.046	0.173	0.072
HFC-227	0.034	0.043	0.018	0.025	0.159	0.063	0.020	0.047	0.051
HFC-125	0.121	0.117	0.044	0.013	0.018	0.014	0.007	0.091	0.053
FC-116	0.124	0.087	0.025	0.033	0.157	0.012	0.063	0.013	0.064
HFC-134a	0.021	0.025	0.024	0.002	0.039	0.061	0.048	0.091	0.039
HFC-236	0.024	1.895	0.030	0.030	0.028	0.015	0.090	0.043	0.269
FC-C318	0.040	0.602	0.065	0.054	0.072	0.014	0.109	0.035	0.124
FC-218	0.083	0.048	0.011	0.050	0.032	0.021	0.044	0.080	0.046
HFC-32/125	0.033	0.324	0.022	0.037	0.217	0.140	0.035	0.122	0.116
NaHCO3	0.297	0.501	0.022	0.047	0.235	0.263	0.042	0.168	0.197
Alloy Avg.	0.078	0.327	0.035	0.035	0.141	0.066	0.055	0.187	

error propagation techniques (Bevington, 1969). Many of these ranges include zero which indicates that we cannot conclude at this level of confidence that the corrosion rate is a value other than zero. On the other hand, scale formation and spalling off of this scale will increase measurement scatter which could result in an estimated mass change rate range that includes zero. As a result, each agent/alloy combination was given a numerical rating based on the absolute value of the maximum or minimum indicated mass change rate in Table 4 rather than on the mean mass change rate. Table 6 gives the absolute mass change rate range for each numerical rating and the equivalent penetration rate for each alloy for mass loss at the maximum rate for the range, while Table 7 gives the score for each agent/alloy combination. Because on cannot determine the amount of metal reacting for mass increases without information on the chemical composition of the scale, mass increases and decreases were given the same weighting for this analysis. It is believed that this rating basis will result in conservative scores for each agent/alloy combination especially since scale formation usually results in a corrosion rate that decreases with time as the scale inhibits mass transport.

Visual examination confirmed the presence of surface films on many of the samples. These films were very thin and could be detected by a color change in the samples. For these exposures, the films may be the result of reaction with residual gasses, decomposition products or the agents themselves. The formation of salt films when metal are exposed to organic solvents has been observed by other investigators. Mass increases are not uncommon during immersion testing and usually descalling techniques are employed to removed these scales for the determination of the remaining metal. Considerable research has been conducted into the development of techniques for the removal of the scales which form in aqueous solutions without attacking the underlying metal. Even with this

Table 4. Mean Mass Change Rate for Each Alloy in Each Agent for 25 Day Immersion at 150 °C [mg/(square meter•day)

Environment	Nit 40	Al 6061	In 625	304 SS	CDA 172	13-8 Steel	AM 355	AISI 4130	Agent Avg.	Std. Dev.
HCFC-22	2.512	6.550	-4.706	2.401	43.847	-0.477	-1.240	40.731	11.202	19.481
HCFC-124	1.320	3.132	-3.816	-0.525	21.097	-1.224	-2.941	4.563	2.701	7.965
FC-31-10	3.529	7.631	-0.525	8.346	38.108	5.103	3.132	15.771	10.137	12.278
HFC-227	0.127	1.828	-0.795	2.019	28.235	0.986	0.095	4.245	4.593	9.677
HFC-125	-0.159	2.846	0.445	1.940	12.734	2.162	0.413	9.634	3.752	4.770
FC-116	0.079	3.434	0.366	2.099	21.589	3.005	1.987	5.771	4.791	7.021
HFC-134a	0.191	1.876	-1.479	0.986	3.275	1.256	-0.207	3.752	1.206	1.752
HFC-236	0.350	35.468	-0.906	1.113	12.385	1.526	0.095	4.912	6.868	12.321
FC-C318	0.111	16.931	0.254	2.846	6.168	2.416	0.079	4.436	4.155	5.610
FC-218	2.194	5.342	0.731	1.288	10.986	3.990	2.146	5.453	4.016	3.326
HFC-32/125	4.292	8.394	2.083	3.450	32.384	7.043	4.451	3.243	28.040	55.097
NaHCO3	5.660	14.849	1.129	3.752	31.224	11.447	3.704	12.734	10.562	9.690
Alloy Avg.	1.684	9.023	-0.601	2.476	21.836	3.103	0.976	22.852		
Std. Dev.	1.953	9.652	1.973	2.181	13.039	3.480	2.151	45.098		

Positive Values = Scaling
Negative Values = Mass Loss

research, these techniques usually remove some unreacted metal or leave scales of their own which induce an error in this mass measurement. Normally, this mass error is small and insignificant compared to the mass of the scale being removed but, the films on the samples in this study are very thin and the composition could be very different from that formed in aqueous solutions. As a result, descalling was not attempted as a means of estimating the thickness of the scales.

Evaluation of the relative performance of the alloy/agent combinations was hampered by the comparison of mass loss and mass gain measurements. Typically, mass loss measurements are evaluated by assuming that all of the lost mass was the result of corrosion and that no corrosion products were left on the surface to create errors in this determination. Then, the quantity of metal reacting and rate of the reactions can be calculated directly from the mass loss. Similarly, mass gain measurements can be evaluated if the reaction and the reaction products are known and it is assumed that none of the scale spalls off and is lost to the environment. However, when these are not known, evaluation contains greater uncertainties, but it is clear that the relative magnitude of mass change is still related to the reaction rate between the metallic species and the environment.

7.3.1.2 Localized Corrosion (Crevice/Weld Coupon) Exposure Experiments. The weld/crevice coupons were cut open and the corrosion damage in the crevice region was examined. Based on these examinations, the results of these experiments were evaluated in three different ways. First, the type of damage observed for each alloy/environment combinations was categorized into one of five different categories based on the appearance of the overlap region: (1) no visible evidence of attack, (2) light discoloration of surface, (3) moderate discoloration with slight attack visible, (4) substantial discoloration and some attack visible, and (5) attack throughout the overlap region.

Table 5. Maximum and minimum estimated mass change rate at 90% confidence level based on the three measurements for each alloy/agent combination and standard statistical error estimation techniques (mg((m^2•day))

Environment	Nit 40	Al 6061	In 625	304 SS	CDA 172	13-8 Steel	AM 355	AISI 4130
HCFC-22	4.418	9.290	-2.587	3.770	51.856	0.570	-0.037	71.660
	0.606	3.810	-6.825	1.031	35.837	-1.524	-2.443	9.801
HCFC-124	2.416	5.325	-2.654	0.452	28.206	0.511	-0.444	6.955
	0.223	0.939	-4.977	-1.501	13.987	-2.959	-5.438	2.171
FC-31-10	4.506	9.530	0.163	9.199	40.691	6.795	4.231	19.957
	2.553	5.732	-1.213	7.494	35.524	3.412	2.033	11.584
HFC-227	0.942	2.867	-0.351	2.613	32.087	2.506	0.585	5.387
	-0.687	0.790	-1.238	1.425	24.383	-0.535	-0.394	3.103
HFC-125	2.758	5.661	1.518	2.265	13.162	2.497	0.581	11.824
	-3.076	0.030	-0.627	1.614	12.306	1.827	0.246	7.445
FC-116	3.068	5.532	0.959	2.892	25.389	3.295	3.499	6.094
	-2.909	1.335	-0.228	1.305	17.790	2.714	0.476	5.448
HFC-134a	0.694	2.480	-0.898	1.032	4.219	2.724	0.944	5.945
	-0.312	1.271	-2.059	0.939	2.331	-0.212	-1.358	1.559
HFC-236	0.932	81.249	-0.190	1.835	13.070	1.877	2.276	5.960
	-0.233	-10.312	-1.622	0.391	11.699	1.175	-2.085	3.865
FC-C318	1.072	31.476	1.835	4.155	7.900	2.752	2.709	5.288
	-0.849	2.387	-1.326	1.536	4.437	2.081	-2.550	3.583
FC-218	4.188	6.503	0.990	2.490	11.752	4.508	3.202	7.375
	0.200	4.180	0.472	0.085	10.219	3.473	1.090	3.531
HFC-32/125	5.098	16.217	2.619	4.348	37.627	10.416	5.305	6.183
	3.487	0.571	1.546	2.552	27.141	3.670	3.598	0.303
NaHCO3	12.843	26.941	1.653	4.880	36.903	17.800	4.711	16.800
	-1.524	2.757	0.605	2.623	25.544	5.094	2.697	8.669

Table 8 gives the results of this analysis, and the only alloy to show category five attack was the 4130 steel which received a five rating in HCFC-22 and HCFC-124. This table also gives the average rating for each agent and ranking of the agents based on this average rating. The lowest rated agents on this basis were HCFC-22 (agent average=3.143), sodium bicarbonate (agent average=3.125), and

Table 6. Mass Change Rate Values Used in Rating Alloy/Agent Behavior in Mass Change Measurements and equivalent penetration rate based on alloy nominal density

Score	Mass Chg Rate mg/(m^2•d)		Equivalent Penetration Rate for Upper Boundary μm/year							
	Lower Bound	Upper Bound	Nit 40	Al 6061	In 625	304 SS	CDA 172	13-8 Steel	AM 355	AISI 4130
1	0	0.1487	0.0069	0.0201	0.0064	0.0068	0.0066	0.0070	0.0069	0.0069
2	0.1487	0.923	0.0431	0.1249	0.0399	0.0425	0.0410	0.0434	0.0426	0.0429
3	0.923	5.00	0.2332	0.6764	0.2164	0.2300	0.2219	0.2353	0.2309	0.2326
4	5.00	25.00	1.166	3.382	1.082	1.150	1.109	1.177	1.154	1.163
5	25.00	125	5.831	16.909	5.409	5.750	5.547	5.883	5.772	5.816
6	125	600	27.99	81.16	25.96	27.60	26.63	28.24	27.70	27.92
7	600	3,000	139.9	405.8	129.8	138.0	133.1	141.2	138.5	139.6
8	3,000	15,000	699.7	2029.1	649.1	690.0	665.7	706.0	692.6	697.9
9	15,000	75,000	3498	10146	3246	3450	3328	3530	3463	3490
10	75,000	∞	∞	∞	∞	∞	∞	∞	∞	∞

(Rating is based on absolute value of mass change rate and penetration rate is only valid for mass loss.)

HFC-227 (agent average=2.750). The best rated agents by this technique were HFC-236 (agent average=1.750), FC-31-10 (agent average=1.875), and HFC-134a (agent average=2.0). However, one should keep in mind that agent averages can be adversely influenced by a single rating, when in service, that specific alloy/agent combination could be avoided and the agent would serve satisfactorily. On this basis, only five of the twelve agents did not have an alloy where no evidence of attack was observed (a one rating) and all of the agents had at least three alloys where only slight discoloration was observed (a two rating). As a result, the crevice/weld immersion experiments show that while there is a clear difference in the corrosivity of the agents, it should be possible to find container alloys for each of the candidates.

While a visual rating of the appearance is a fair estimate of the relative corrosivity of each agent, there are numerous cases where several alloy/agent combinations received the same rating and there is no indication of which agent was more or less corrosive for a specific alloy. As a result, all of the weld/crevice samples of each alloy were compared to each other and the agents were ranked based on the appearance of the corrosion damage in the crevice region for each alloy. Each agent was given a score between one and twelve for each alloy where one showed less evidence of corrosion damage than two and so forth. This analysis allows the identification of the least corrosive agent for each alloy and the results are given in Table 9. The data in this table indicates the same general trend as Table 8 with the low ranking agents in Table 8 receiving most of the lower rankings; but since there is no relationship between the scores from one agent to another (*e.g.*, an eight for one agent/alloy combination may have less attack than a much lower rating for another combination), this table should

Table 7. Mass Loss Rate Evaluation of Agents and Alloys based on 25 Day Immersion at 150 °C

Environment	Nit 40	Al 6061	In 625	304 SS	CDA 172	13-8 Steel	AM 355	AISI 4130	Agent Avg.	Std. Dev.	Agent Rank
HCFC-22	3	4	3	3	5	2	3	5	3.50	1.07	9
HCFC-124	3	3	3	2	4	3	3	3	3.00	0.53	7
FC-31-10	3	4	2	4	5	4	3	4	3.63	0.92	11
HFC-227	1	3	2	3	5	3	1	3	2.63	1.30	1
HFC-125	2	3	2	3	4	3	2	4	2.88	0.83	4
FC-116	1	3	2	3	4	3	3	4	2.88	0.99	4
HFC-134a	2	3	3	3	3	3	2	3	2.75	0.46	3
HFC-236	2	5	2	3	4	3	1	3	2.88	1.25	4
FC-C318	1	4	2	3	4	3	1	3	2.63	1.19	1
FC-218	3	4	2	3	4	3	3	4	3.25	0.71	8
HFC-32/125	3	4	3	3	5	4	3	3	3.50	0.76	9
NaHCO3	4	4	3	3	5	4	3	4	3.75	0.71	12
Alloy Avg.	2.33	3.67	2.42	3.00	4.33	3.17	2.33	3.58			
Std. Dev.	0.98	0.65	0.51	0.43	0.65	0.58	0.89	0.67			
Alloy Rank	1	7	3	4	8	5	1	6			

Score	Freq	
1	6	No evidence of attack ($t<0.741$, 50% CI).
2	14	Some inconclusive evidence of attack (0.741(50% CI) $< t <$ 4.6 (99% CI)).
3	47	Conclusive evidence of attack ($t>4.6$, 99% CI).
4	22	Corrosion of little concern, (less than ≈ 1 μm/year, 3μm for Al alloy).
5	7	Corrosion may be a concern
6	0	Corrosion rate should be considered in design
7	0	Corrosion about 1 to 5 mils per year
8	0	Rapid Corrosion
9	0	Very rapid corrosion
10	0	Extremely rapid corrosion

only be used for identifying the relative corrosivity of each agent to a specific alloy. However, it is worthy of note that sodium bicarbonate ($NaHCO_3$) received a twelve rating for half of the alloys and a ten or higher rating for six of the eight alloys.

Perhaps a more valuable comparison would be a comparison of the performance of the alloy in a given agent, Table 10. As with Table 9, this ranking was developed by a side by side comparison of the crevice/weld region of the samples only this time the different alloys tested in the same agent were compared. This ranking allows for identification of the alloy which is more resistant to attack in the crevice and weld heat affected zone by each agent. Again, a low rating in one alloy/environment combination may be considerably better than a higher rating in another combination

Table 8. Weld/Crevice Coupon Visual Classification of Attack After 25 Day Immersion at 150 °C

Environment	Nit 40	Al 6061	In 625	304 SS	CDA 172	13-8 Steel	AM 355	AISI 4130	Agent Avg.	Std. Dev.	Agent Rank
HCFC-22	2	2	2	3	4	3	3	5	3.14	1.07	12
HCFC-124	2	2	1	2	3	3	3	5	2.63	1.19	8
FC-31-10	1	1	2	2	2	2	2	3	1.88	0.64	2
HFC-227	2	2	2	3	3	3	3	4	2.75	0.71	10
HFC-125	2	2	2	2	3	2	3	2	2.25	0.46	5
FC-116	2	2	1	2	2	3	2	3	2.13	0.64	4
HFC-134a	1	1	1	2	2	3	4	2	2.00	1.07	3
HFC-236	2	2	1	1	2	2	2	2	1.75	0.46	1
FC-C318	2	3	2	2	2	2	2	4	2.38	0.74	6
FC-218	3	4	2	2	2	2	2	4	2.63	0.92	8
HFC-32/125	3	2	1	2	2	2	3	4	2.38	0.92	6
NaHCO3	2	3	2	2	4	4	4	4	3.13	0.99	11
Alloy Avg.	2.00	2.17	1.58	2.08	2.58	2.58	2.75	3.50	2.42		
Std. Dev.	0.60	0.83	0.51	0.51	0.79	0.67	0.75	1.09	0.45		
Alloy Rank	2	4	1	3	5	5	7	8	0.45		

Classification Criteria
1=No visible staining
2=Light Staining in overlap region
3=Moderate staining with slight attack visible in overlap region.
4=Substantial staining with moderate attack in overlap region.
5=Heavy attack throughout overlap region.

so comparisons between environments should not be done with this data, but this tabulates the results of a direct visual comparison of the different alloy's performance in each agent.

7.3.1.3 Environmental Induced Fracture Experiments (Slow Strain Rate Tensile Tests). Slow strain rate tensile tests result in three parameters that can be used as an indicator of environmental induced fracture. First, the ultimate tensile strength (UTS) is a measure of the fracture strength of the sample and it is determined from the maximum load observed during the tensile test according to the relationship:

$$UTS = \frac{P_{max}}{A_o} \tag{3}$$

where P_{max} is the maximum load supported by the sample during the test and A_0 is the initial cross-sectional area of the gage section of the sample. Environmental interactions that lower the strength of the sample either by corrosion, cracking or other interaction will result in a change in this parameter. Environments can also interact with deformation occurring at surfaces and at crack tips in the sample to limit ductility and cause cracking. So, a second indicator of environmental induced fracture is total strain to cause failure (ϵ_f) which is determined from the relationship

$$\epsilon_f = \frac{\ell_f - \ell_o}{\ell_o} \tag{4}$$

Table 9. Weld/Crevice Coupon Visual Ranking of Agents for Each Alloy After 25 Day Immersion at 150 °C

Environment	Nit 40	Al 6061	In 625	304 SS	CDA 172	13-8 Steel	AM 355	AISI 4130	Agent Avg.	Std. Dev.
HCFC-22	4	4	7	12	11	9	9	11	8.38	3.11
HCFC-124	3	3	3	8	10	7	8	12	6.75	3.45
FC-31-10	1	1	6	4	1	2	3	5	2.88	1.96
HFC-227	8	7	8	11	9	8	5	7	7.88	1.73
HFC-125	5	5	9	7	8	5	10	4	6.63	2.20
FC-116	7	6	4	9	4	11	4	2	5.88	3.00
HFC-134a	2	2	2	10	7	10	11	1	5.63	4.31
HFC-236	6	9	5	1	2	6	6	3	4.75	2.60
FC-C318	9	11	10	3	6	3	1	9	6.50	3.78
FC-218	11	12	11	2	5	1	2	8	6.50	4.57
HFC-32/125	12	8	1	5	3	4	7	10	6.25	3.69
NaHCO3	10	10	12	6	12	12	12	6	10.00	2.62

1 = Best Performance

where l_f is the total change in sample length during the experiment and l_0 is the initial gage length. This value includes the elastic and plastic strains required to cause failure. Another means for measuring the ductility of the sample is the reduction in area (RA) which is a third means for indicating environmentally induced fracture. The RA is determined by measuring the area of the fracture surface after the test is completed and the relationship

$$RA = \frac{A_f - A_o}{A_o} \tag{5}$$

where A_f is the cross sectional area of the fracture surface and A_0 is the initial gage section cross sectional area. This measurement includes only the plastic deformation required to cause failure and for some alloys is a better measure of environmental interactions than the strain to failure. Typically, these parameters are analyzed by forming a ratio of the value observed in the environment to observed in a reference environment (usually an inert environment). Another approach to analysis is to estimate the statistical significance of the difference between the mean determined for the parameter in the inert reference environment and the mean determined for the agent. The significance of this difference is determined by dividing the difference in the means by the standard deviation estimated for that parameter for that specific alloy and temperature in this type of test.

Table 10. Weld/Crevice Coupon Visual Ranking of Alloys for Each Agent After 25 Day Immersion at 150 °C

Environment	Nit 40	Al 6061	In 625	304 SS	CDA 172	13-8 Steel	AM 355	AISI 4130
HCFC-22	1	2	3	4	7	5	6	8
HCFC-124	3	2	1	4	7	5	6	8
FC-31-10	2	1	3	4	5	6	7	8
HFC-227	3	1	2	4	6	7	5	8
HFC-125	3	4	2	1	7	5	8	6
FC-116	2	3	1	4	6	8	5	7
HFC-134a	2	3	1	4	6	7	8	5
HFC-236	4	3	1	2	5	7	6	8
FC-C318	2	7	3	1	6	5	4	8
FC-218	4	7	2	1	6	3	5	8
HFC-32/125	6	3	1	2	4	5	7	8
NaHCO3	2	4	3	1	8	5	6	7
Alloy Avg.	2.83	3.33	1.92	2.67	6.08	5.67	6.08	7.42
Std. Dev.	1.34	1.97	0.90	1.44	1.08	1.37	1.24	1.00

1 = Best Performance

Tables 11 and 12 gives the average UTS determined for each alloy in air at room temperature, argon at 150 °C, and each agent at 150 °C. The ratio of the average UTS in each agent to the average UTS in Ar at the same temperature is given in Table 13. In this table, it can be seen that for 87 of the 96 agent alloy combinations the UTS ratio is $1.00 \pm .05$. For the nine outside this range, two have a higher average UTS in the agent than in Ar. Of the seven with a lower average UTS in the agent, only two is more than 10% below the value determined in Ar: 304 and 4130 steel in FC-C318. Table 14 gives the results of an estimate of the significance of the differences. A significant decrease in the average UTS may be an indication of cracking, but it could also be due to corrosion reactions reducing effective cross-section or a flaw in the sample. An increase in the average UTS is unusual and this indicates that sample/environment interactions are inhibiting deformation and fracture, but it could also indicate a interference between the corrosion products being generated on the sample and the seal of the autoclave through which the sample must slide. The most important point is that no agent caused significant changes in all alloys indicating that materials for the containment and reliable distribution of any of these candidates can be identified.

The ductility results for the SSR tests are given in Tables 15-20. Table 15 gives the average strain to failure for each alloy/environment combination, laboratory air at room temperature and Ar at 150 °C. Table 16 gives the ratio of the average strain to failure for each alloy in each environment to that observed in the same alloy in Ar at the same temperature and Table 17 gives the statistical

Table 11. Average Ultimate Tensile Strength in Each Agent at 150 °C as Compared to Ar at 150 °C and Air at 25 °C (MPa)

Environment	Nit 40	Al 6061	In 625	304 SS	CDA 172	13-8 Steel	AM 355	AISI 4130
Air, 25 °C	727	341	957	773	763	1117	1005	673
Ar, 150 °C	610	240	927	667	874	1136	969	647
HCFC-22	602	232	892	674	855	1155	938	624
HCFC-124	624	235	937	648	860	1027	945	665
FC-31-10	619	235	910	649	841	1176	935	673
HFC-227	610	235	911	667	865	1156	928	650
HFC-125	611	235	924	650	847	1154	917	669
FC-116	599	221	880	638	830	1163	922	629
HFC-134a	618	225	932	653	851	1144	929	688
HFC-236	612	245	930	633	861	1168	935	648
FC-C318	597	289	924	550	851	1182	950	558
FC-218	624	235	944	681	842	1170	928	663
HFC-32/125	624	225	886	622	843	1138	919	631
NaHCO3	623	252	947	643	852	1217	953	674
Alloy Avg.	614	239	918	642	850	1154	933	648
Std. Dev*.	16	16	22	37	22	44	15	35

Alloy Avg. Average of the means determine for each of the agents.
Std. Dev.* The "Alloy Standard Deviation" was estimated from the Ar at 150 °C tests

analysis of the significance of this difference. In Table 16, it can be seen that measured strain to failure increased for most of the alloy/environment combinations indicating the deformation was easier in these environments than in Ar. Environmentally induced cracking, or stress corrosion cracking (SCC), is usually indicated by a reduction in ductility. Of the 96 alloy environment combinations, the strains to failure of three of the alloy/environment combinations were more than 10% less than that observed in Ar: Nit 40 in HCFC-124 (0.87), Nit 40 in FC-31-10 (0.88), and Nit 40 in HFC-236 (0.88). However, these strain to failure measurements are based on load frame displacement measurements taken by a transducer outside of the autoclave during the experiment. As a result, the reduction in area measurements which are based on measurement of the fracture surface are in an optical microscope after the experiment are a more reliable indication of changes in ductility. Table 18 presents this data for each alloy in laboratory air at 25 °C, Ar gas at 150 °C and each agent at 150 °C. Table 19 gives the ratio of the average reduction in area measured for each alloy/agent combination to Ar at 150 °C and the statistical significance of this difference is given in Table 20. In Table 19, it can be seen that the reduction in area is reduced by more than 5% in 11 of

Table 12. Average Ultimate Tensile Strength in Each Agent at 150 °C as Compared to Ar at 150 °C and Air at 25 °C (ksi)

Environment	Nit 40	Al 6061	In 625	304 SS	CDA 172	13-8 Steel	AM 355	AISI 4130
Air, 25°C	105.4	49.4	138.8	112.1	110.7	162.0	145.7	97.6
Ar, 150°C	88.5	34.8	134.4	96.7	126.7	164.7	140.5	93.8
HCFC-22	87.3	33.6	129.4	97.7	123.9	167.5	136.0	90.4
HCFC-124	90.5	34.1	135.9	93.9	124.8	149.0	137.1	96.4
FC-31-10	89.7	34.1	131.9	94.2	122.0	170.6	135.7	97.7
HFC-227	88.5	34.0	132.2	96.7	125.4	167.6	134.6	94.3
HFC-125	88.6	34.1	134.0	94.3	122.9	167.4	133.0	97.0
FC-116	86.9	32.1	127.6	92.5	120.3	168.6	133.7	91.2
HFC-134a	89.7	32.6	135.2	94.7	123.4	165.9	134.7	99.8
HFC-236	88.8	35.5	134.9	91.8	124.8	169.5	135.6	94.0
FC-C318	86.6	41.9	134.1	79.8	123.4	171.4	137.8	80.9
FC-218	90.5	34.1	136.9	98.8	122.1	169.6	134.5	96.1
HFC-32/125	90.5	32.6	128.4	90.2	122.2	165.0	133.2	91.5
NaHCO3	90.3	36.5	137.4	93.3	123.6	176.5	138.1	97.8
Alloy Avg.	89.0	34.6	133.2	93.2	123.2	167.4	135.3	93.9
Std. Dev.*	2.3	2.3	3.2	5.3	3.2	6.4	2.2	5.1

Alloy Avg. = Average of the means determine for each of the agents.
Std. Dev.* = The "Alloy Standard Deviation" was estimated from the Ar at 150°C tests

the 96 alloy/agent combinations and is reduced by more than 10% in only four alloy/agent combinations: Al 6061 in HCFC-124 (0.85), Al 6061 in $NaHCO_3$ (0.83), SS 304 in $NaHCO_3$ (0.83), and AISI 4130 in $NaHCO_3$ (0.87). Since three of these five are with the same agent, $NaHCO_3$, this agent may have problems with this failure mode.

To summarize the results of the SSR tensile tests, Table 21 was assembled by taking the highest (worst) score received by each agent/alloy combination in Tables 14, 17, and 20 (UTS, strain to failure and RA) and assigning a number to each agent/alloy combination. Since the agent/alloy scores given in these tables are the absolute value of the difference between the mean for the alloy in the agent and Ar divided by the standard deviation for this alloy and parameter at 150 °C, this rating is a measure of the significance of any postulated environmental influence on the deformation and fracture of the agent/alloy combinations. If the maximum deviation was less than one standard deviation, the agent/alloy combination was assigned a value of one, if it was greater than one standard deviation, but less than two, it was assigned a two and so on. In Table 21, it can be seen that 65 of the 96 agent/alloy combinations received a one or two rating. Every agent had at least one alloy with a one rating and only two agents had only one alloy with a rating of one.

Table 13. Average Ultimate Tensile Strength Ratios [(Mean for Envir.)/(Mean for Hot Ar)]

Environment	Nit 40	Al 6061	In 625	304 SS	CDA	13-8 Steel	AM355 SS	AISI 4130	Agent Avg.
HCFC-22	0.99	0.97	0.96	1.01	0.98	1.02	0.97	0.96	0.96
HCFC-124	1.02	0.98	1.01	0.97	0.98	0.90	0.98	1.03	0.98
FC-31-10	1.01	0.98	0.98	0.97	0.96	1.04	0.97	1.04	0.99
HFC-227	1.00	0.98	0.98	1.00	0.99	1.02	0.96	1.00	0.98
HFC-125	1.00	0.98	1.00	0.97	0.97	1.02	0.95	1.03	0.98
FC-116	0.98	0.92	0.95	0.96	0.95	1.02	0.95	0.97	0.98
HFC-134a	1.00	0.94	1.01	0.98	0.97	1.01	0.96	1.06	0.98
HFC-236	1.00	1.02	1.00	0.95	0.99	1.03	0.97	1.00	0.99
FC-C318	0.98	1.20	1.00	0.83	0.97	1.04	0.98	0.86	0.96
FC-218	1.02	0.98	1.02	1.02	0.96	1.03	0.96	1.02	0.99
HFC-32/125	1.02	0.94	0.96	0.93	0.96	1.00	0.95	0.97	0.99
NaHCO3	1.02	1.05	1.02	0.96	0.98	1.07	0.98	1.04	1.01
Alloy Avg.	1.00	1.00	0.98	0.97	0.97	1.01	0.96	0.98	

On the negative side, no alloy received only one's and two's in all of the agents and no agent received only one's and two's for all of the alloys. The best performance by an alloy was demonstrated by the 304 stainless steel alloy which received a one in all except for three of the environments. The best performing agents were HFC-236 and HFC-125 with FC-31-10 coming in third. However, each of these agents received a three or a four rating on at least one alloy. Since the alloys have different chemical compositions, surface films and corrosion susceptibilities, this is not surprising, but it indicates the importance of conducting experiments of this type.

7.3.1.4 Summary of Aircraft Storage and Distribution System Corrosion Experiments. To combine the performance of the different agent/alloy performances on the three different types of tests that comprise this part of the investigation, each agent/alloy combination was given a rating between one and ten based on its performance in that particular test. Table 22 reviews the results for each agent/alloy combination in the three types of experiments that comprise this part of this investigation: Mass Change Exposure Experiments (Exp.), Localized Corrosion Exposure Experiments (Crevice) and Environmental Induced Fracture (SSR). To allow for ready comparison between these results, a similar rating scheme was adopted for each of the three different types of tests used in this part of this study. Basically, this scheme assigned a numerical score between one and ten to each agent/alloy combination investigated in that particular test. Whenever possible, a numerical rule was used for the rating scheme with the magnitude of the standard deviation used to distinguish between one, two, and three while order of magnitude steps were used from six to 10. The interpretation of the meaning of the numerical ratings is given at the bottom of Table 22. Basically, a one indicates no discernable evidence of attack, a five indicates attack that may be a problem, and a ten indicates extremely rapid

Table 14. Score for the Average Ultimate Tensile Strength|[(Mean for Envir.)-(Mean for Hot Ar)]/(Alloy Std. Dev.)|

Environment	Nit 40	Al 6061	In 625	304 SS	CDA 172	13-8 Steel	AM355 SS	AISI 4130	Agent Avg.
HCFC-22	0.49	0.53	1.57	0.18	0.88	0.43	2.06	0.67	0.85
HCFC-124	0.89	0.30	0.47	0.52	0.61	2.45	1.55	0.50	0.91
FC-31-10	0.55	0.34	0.79	0.48	1.49	0.91	2.20	0.76	0.92
HFC-227	0.00	0.35	0.70	0.00	0.41	0.45	2.70	0.09	0.59
HFC-125	0.04	0.31	0.13	0.46	1.20	0.41	3.41	0.62	0.82
FC-116	0.68	1.22	2.13	0.79	2.01	0.60	3.11	0.51	1.38
HFC-134a	0.52	0.97	0.23	0.38	1.03	0.17	2.64	1.17	0.89
HFC-236	0.14	0.29	0.13	0.93	0.59	0.73	2.23	0.02	0.63
FC-C318	0.80	3.14	0.12	3.19	1.04	1.04	1.24	2.55	1.64
FC-218	0.89	0.33	0.76	0.39	1.46	0.76	2.73	0.45	0.97
HFC-32/125	0.87	1.00	1.87	1.23	1.42	0.05	3.33	0.46	1.28
NaHCO3	0.79	0.74	0.92	0.65	0.99	1.83	1.07	0.78	0.97
Alloy Avg.	0.56	0.79	0.82	0.77	1.09	0.82	2.36	0.71	

attack. A rating above four indicates more than just superficial corrosion and a better understanding of the attack responsible for this score should be developed before putting these combinations in service.

From Table 22, it can be seen that some agent/alloy combinations that did well in one test did poorly in another. For example, AISI 4130 steel performed well in the SSR tests in all of the agents, but did poorly in most of the other tests. On the other hand, some of the alloys which apparently retain passivity in the agents, had some indications of problems in the SSR tests such as 304 stainless steel in FC-C318. The results of these tests can be combined into a single overall rating number for each agent/alloy combination by either averaging the results of the tests, Table 23, or by taking the worst rating achieved for the three tests as the overall rating, Table 24. Since a good rating on two of the tests could bring an unacceptable rating on one of the tests into the acceptable range for the overall rating based on averaging, it was decided that an overall rating which is the worst rating received on the three different tests was the best way to evaluate the overall performance of an agent/alloy combination, Table 24. By examining this table, it can be seen that by this rating scheme the best rated agents are HFC-134a with HFC-227, HFC-125 and HFC-236 not far behind. None of the agents received an agent average rating for the eight alloys higher than five, but $NaHCO_3$ was over four. Also, all of the agents had at least two alloys with a three or lower rating. That is, none of the agents were so corrosive that an alloy could not be identified for aircraft storage and distribution systems, but clearly some agents were less aggressive than others and some agent/alloy combinations may be undesirable. The origin of the differences in the corrosivity of the agents could be due to reactions between the metals and the agents or it could be due to different contamination or

Table 15. Average Strain to Failure in Each Agent at 150 °C (Except lab air which was at room temperature) (%)

Environment	Nit 40	Al 6061	In 625	304 SS	CDA 172	13-8 Steel	AM355 SS	AISI 4130
Lab Air	49.9	13.0	44.4	30.3	13.0	5.9	10.7	8.3
Hot Ar	41.5	7.9	41.0	13.6	10.1	6.2	9.2	7.9
HCFC-22	37.8	8.9	37.7	12.5	12.4	7.5	9.8	8.9
HCFC-124	36.0	10.5	43.7	14.1	12.4	7.9	9.1	8.2
FC-31-10	36.7	10.1	37.2	12.4	12.9	6.5	7.8	8.0
HFC-227	37.8	10.7	42.6	13.6	11.7	6.9	9.6	7.7
HFC-125	40.4	9.8	43.4	15.1	11.6	6.7	9.8	8.1
FC-116	40.5	9.6	46.5	17.1	12.2	6.9	9.1	8.8
HFC-134a	37.7	9.4	46.5	12.7	10.1	7.7	9.2	7.8
HFC-236	36.3	9.7	41.5	16.9	9.7	7.0	9.7	8.2
FC-C318	41.7	8.5	43.1	36.0	12.8	8.1	9.1	9.6
FC-218	41.0	9.1	45.0	15.0	11.7	6.6	9.0	9.5
HFC-32/125	39.4	9.2	46.2	17.4	11.6	7.2	9.6	8.5
NaHCO3	42.5	7.5	46.0	17.4	11.6	10.5	9.5	7.5
CF3I	40.6	8.6	47.8	21.3	11.0	7.4	8.0	6.8
Alloy Avg.	39.3	9.3	43.4	16.8	11.6	7.4	9.2	8.3
Std. Dev.*	3.0	1.2	2.6	5.5	1.6	0.9	0.6	0.7

Alloy Avg. Average of the means determine for each of the agents.
Std. Dev.* The "Alloy Standard Deviation" was estimated from the Ar at 150 °C tests

residual levels in the agents. If the corrosivity is due to contaminants and residuals, then changes in processing or storage that alters these levels would also alter the corrosivity of the agents. Additional testing will be required to determine the cause of the observed corrosion behaviors and the role of contaminants and residuals in determining the corrosivity.

7.3.2 Post-Deployment Corrosion.

7.3.2.1 Literature Review of Corrosion of Metals in Halide Ions. All of the fire suppressants investigated in this study except for $NaHCO_3$, contain fluoride and produce fluoride ions and HF during combustion. Since other halogens are also incorporated in these, and other potential fire suppressants, other halogen acids will be produced by combustion of these suppressants. Therefore, the post-deployment corrosion damage to aircraft materials will depend on the corrosivity of surface films containing these species on the metals of the aircraft frame, engine components, etc.

Table 16. Average Strain to Failure Ratio in Each Agent at 150 °C [(Agent)/(Hot Ar)]

Environment	Nit 40	Al 6061	In 625	304 SS	CDA 172	13-8 Steel	AM355 SS	AISI 4130	Agent Avg.
HCFC-22	0.91	1.12	0.92	0.92	1.23	1.20	1.06	1.13	1.01
HCFC-124	0.87	1.32	1.06	1.04	1.23	1.28	0.99	1.03	1.10
FC-31-10	0.88	1.27	0.91	0.91	1.28	1.05	0.85	1.01	0.96
HFC-227	0.91	1.34	1.04	1.00	1.17	1.11	1.05	0.97	1.13
HFC-125	0.97	1.24	1.06	1.11	1.16	1.08	1.06	1.02	1.14
FC-116	0.98	1.21	1.13	1.26	1.21	1.11	0.99	1.12	1.06
HFC-134a	0.91	1.19	1.13	0.93	1.00	1.24	1.00	0.99	1.09
HFC-236	0.88	1.23	1.01	1.25	0.97	1.13	1.05	1.03	1.13
FC-C318	1.00	1.07	1.05	2.65	1.27	1.30	0.99	1.22	1.13
FC-218	0.99	1.14	1.10	1.11	1.17	1.06	0.97	1.20	1.14
HFC-32/125	0.95	1.16	1.13	1.28	1.15	1.16	1.04	1.08	1.11
NaHCO3	1.03	0.94	1.12	1.29	1.15	1.70	1.03	0.95	1.21
Alloy Avg.	0.94	1.19	1.05	1.23	1.17	1.20	1.01	1.06	

Most engineering alloys that exhibit good corrosion resistance do so due to the formation of a "passivating" surface film. Aluminum alloys and stainless steels are excellent examples of alloys based on active elements that behave in a relatively noble manner due to the formation of continuous protective corrosion product films. These films are usually oxides, hydroxides or oxide-hydroxide mixtures. These surface films may be crystalline and they may be precipitated out of the solution adjacent to the metals surface, but it is generally believed that the more rapidly grown, amorphous films are more protective than precipitated crystalline films. No matter what the nature of the surface film, it is generally found that halogen ions in the environment and on these films tend to destabilize the protective passivating films. Presumably, this is because the soluble metal-halide salt is thermodynamically preferred over the relatively insoluble metal-oxide or hydroxide compounds in the passive film at the passive film to environment interface. This is a very simplified view which ignores many kinetic issues in passive film growth and breakdown, but many of the essential details in the relationship between halogen ions and passivity breakdown can be understood based on this simple model: (1) increasing halide ion activity reduces passive film stability, (2) the more aggressive halide is the more electronegative ($F^- > Cl^- > Br^- > I^- > At^-$), (3) pH influences stability, (4) electrode potential influences stability and (5) metal-halide salt solubility should exhibit an influence.

Aluminum alloys are the most common metallic alloy type used in airframe construction and the most susceptible to pitting by halide ions of the metals of concern so this review will focus on the effect of halide ions on the corrosion behavior of these alloys. Aluminum is a relatively active element and aluminum alloys corrode as rapidly as mass transport to the surface will allow if the passive film becomes unprotective for any reason. As a result, aluminum alloys are not used in environments where passivity is not maintained (*e.g.*, $pH < 4$ or $pH > 10$). However, pitting, crevice

Table 17. Score for the Average Strain to Failure |[(Mean for Envir.)-(Mean for Hot Ar)]/(Alloy Std. Dev.)|

Environment	Nit 40	Al 6061	In 625	304.00 SS	CDA 172	13-8 Steel	AM355 SS	AISI 4130	Agent Avg.
HCFC-22	1.22	0.78	1.29	0.20	1.44	1.47	0.97	1.51	1.11
HCFC-124	1.80	2.10	1.02	0.10	1.46	2.04	0.17	0.42	1.14
FC-31-10	1.57	1.79	1.47	0.22	1.76	0.34	2.26	0.10	1.19
HFC-227	1.21	2.26	0.61	0.01	1.03	0.81	0.69	0.31	0.87
HFC-125	0.36	1.55	0.90	0.28	0.97	0.60	0.97	0.23	0.73
FC-116	0.32	1.35	2.10	0.64	1.32	0.81	0.18	1.39	1.01
HFC-134a	1.23	1.22	2.11	0.16	0.02	1.78	0.00	0.14	0.83
HFC-236	1.69	1.49	0.18	0.61	0.21	0.96	0.79	0.41	0.79
FC-C318	0.07	0.49	0.78	4.11	1.68	2.19	0.19	2.61	1.51
FC-218	0.17	0.95	1.51	0.27	1.03	0.44	0.44	2.45	0.91
HFC-32/125	0.66	1.06	1.98	0.69	0.95	1.15	0.59	0.90	1.00
NaHCO3	0.35	0.40	1.90	0.71	0.94	5.09	0.48	0.66	1.32
Alloy Avg.	0.89	1.29	1.32	0.67	1.07	1.47	0.64	0.93	

corrosion or stress corrosion cracking may result in environments where aluminum is normally passive if halide ion concentrations exceed critical values.

As discussed above, when aluminum is exposed to solutions containing different types of halide ions, passive film breakdown and pitting should vary with the electronegativity of the halide ion. Chloride, bromide and iodide follow this trend, but fluoride was found to be less aggressive to aluminum alloys than chloride and bromide (Davies and Prigmore 1984). Since aluminum salts formed with fluoride are less soluble than other aluminum halide salts, several investigators have postulated that this difference is due to the formation of different types of salt films (Zotikov, Bakhmutova *et al.* 1974; Davies and Prigmore 1984). In general, aluminum alloys have excellent atmospheric corrosion resistance and, in most atmospheres, the corrosion rate of aluminum decreases with time as the passive film become thicker (Fink and Boyd 1970; Bailey, Porter *et al.* 1976). However, cyclic wetting and drying and the presence of aggressive species in the atmosphere can accelerate attack by damaging the passivating film. Marine and coastal environments with their high humidity and particulates rich in chloride ions can be particularly aggressive. Also, gases such as sulfur dioxide (SO_2) chlorine (Cl_2) and hydrogen chloride gas have been found to be aggressive for aluminum alloys (Bailey, 1976; Scully, 1990(a)).

7.3.2.2 Post-deployment Corrosion Test Results. The results of the post-deployment corrosion tests are shown in Figures 7 through 14 for Alloy 6061-T6, AISI 4130, 13-8 Mo steel, AM 355, 304 stainless steel, Nitronic 40, Inconel 625, and CDA 172 (Cu-Be) respectively. The data in these figures are for 30 days of exposure at three different humidities (20, 52 and 93% RH) following

Table 18. Average Reduction in Area in Each Agent at 150 °C (Except lab air which was at room temperature) (%)

Environment	Nit 40	Al 6061	In 625	304 SS	CDA 172	13-8 Steel	AM355 SS	AISI 4130
Lab Air	78.1	50.9	73.7	76.7	66.3	69.4	48.6	52.1
Hot Ar	79.2	42.3	69.5	67.8	27.5	60.0	48.6	50.8
HCFC-22	79.3	40.2	65.7	67.9	38.7	61.5	49.3	50.4
HCFC-124	79.6	35.8	65.7	71.7	36.6	56.2	48.3	48.7
FC-31-10	80.2	40.0	64.2	70.2	37.8	60.5	51.4	47.6
HFC-227	79.5	39.1	68.9	69.8	43.3	61.1	48.7	48.2
HFC-125	80.4	39.4	67.3	68.7	40.0	61.9	48.6	49.2
FC-116	79.6	41.1	69.6	71.9	40.5	62.5	48.5	49.2
HFC-134a	80.3	39.0	69.9	69.0	31.1	59.6	50.4	49.6
HFC-236	79.1	40.7	65.7	72.6	32.9	60.1	48.6	49.1
FC-C318	79.5	40.9	70.3	68.6	36.3	61.1	47.5	49.5
FC-218	86.2	42.2	69.3	70.8	31.4	59.5	47.2	47.5
HFC-32/125	79.5	40.9	67.0	72.5	37.9	62.3	48.5	50.1
NaHCO3	80.1	35.2	68.4	56.3	33.8	58.1	51.5	44.3
Alloy Avg.	80.2	39.8	67.8	69.1	36.0	60.3	49.1	48.8
Std. Dev.*	2.3	2.3	3.2	5.3	3.2	6.4	2.2	5.1

Alloy Avg. Average of the means determine for each of the agents.
Std. Dev.* The "Alloy Standard Deviation" was estimated from the Ar at 150°C tests

three different surface pretreatments: (1) artificial seawater plus NaF, (2) artificial seawater plus $NaHCO_3/Na_2CO_3$ and (3) artificial seawater plus NaOH. The mass changes (after washing with distilled water) for this exposure period are plotted in these figures as a function of the relative humidity of the exposure environment. In these figures, it can be seen that for most of the alloys and pretreatments, no particular surface pretreatment was consistently worse than the others, that there is no clear trend in the magnitude of the mass change with relative humidity, and that, except for three alloys, the mass changes were almost always small mass losses.

A mass loss indicates the formation of corrosion products that were removed by washing in distilled water prior to weighing of the samples. These products may be either ions in thin electrolyte layers on the surface or solid corrosion products that are dissolved or physically removed by the washing process. In either case, these measurements indicate corrosion of the underlying alloy. However, for all of these alloys the mass changes were <2 mg for these exposures which corresponds to a corrosion rate of <0.024 grams per meter squared per day (0.24 MDD) which is a relatively low corrosion rate. The three exceptions were: aluminum alloy 6061-T6, AISI 4130 steel, and the Cu-Be alloy CDA-172. These alloys exhibited mass increases of a much larger magnitude

Table 19. Average Reduction in Area Ratio in Each Agent at 150 °C [(Agent)/(Hot Ar)]

Environment	Nit 40	Al 6061	In 625	304 SS	CDA 172	13-8 Steel	AM355 SS	AISI 4130	Agent Avg.
HCFC-22	1.00	0.95	0.95	1.00	1.41	1.03	1.00	0.99	1.04
HCFC-124	1.01	0.85	0.95	1.06	1.33	0.94	0.98	0.96	1.01
FC-31-10	1.02	0.95	0.92	1.03	1.37	1.02	1.05	0.94	1.04
HFC-227	1.00	0.92	0.99	1.03	1.58	1.03	0.99	0.95	1.06
HFC-125	1.01	0.93	0.97	1.01	1.45	1.04	0.99	0.97	1.05
FC-116	1.01	0.97	1.00	1.06	1.48	1.05	0.99	0.97	1.06
HFC-134a	1.01	0.92	1.01	1.02	1.13	0.99	1.04	0.98	1.01
HFC-236	1.00	0.96	0.95	1.07	1.20	1.01	0.99	0.97	1.02
FC-C318	1.00	0.97	1.01	1.01	1.32	1.02	0.97	0.98	1.04
FC-218	1.09	1.00	1.00	1.04	1.14	1.00	0.96	0.94	1.02
HFC-32/125	1.00	0.97	0.97	1.07	1.38	1.04	0.99	0.99	1.05
NaHCO3	1.01	0.83	0.99	0.83	1.23	0.97	1.05	0.87	0.97
Alloy Avg.	1.02	0.94	1.00	1.00	1.23	1.05	0.99	1.01	

than the small mass losses of the other five alloys and required the use of a much larger scale for plotting the results for these alloys. For aluminum alloy 6061 (Figure 7), the mass changes ranged from a small mass loss of about 2 mg at 20% RH for the NaOH pretreatment to a mass increase of about 15 mg at 93% RH for the carbonate/bicarbonate pretreatment. The NaF pretreatment showed mass increases between 2 and 6 mg for these exposures. Apparently, adding NaF to the surface electrolyte film was not as detrimental to this alloy as the carbonate/bicarbonate treatment. Since the films were prepared by first spraying with artificial seawater, all of the surface films contained chloride ions which are typically found to be more detrimental than fluoride ions to aluminum alloys. While the NaOH pretreatment resulted in only small mass changes, it should be noted that this pretreatment resulted in the formation of small pits on the surface for the low humidity exposure (20% RH). For the AISI 4130 steel alloy (Figure 8), the carbonate/bicarbonate and the NaOH surface pretreatments resulted in mass changes between -1 mg and 2 mg. However, the NaF pretreatment resulted in the growth of an insoluble corrosion product film as indicated by a mass increase of over 17 mg. Apparently, unlike the aluminum alloy, adding NaF to the thin electrolyte film on the surface of this alloy resulted in significant changes in the corrosivity of this film. For the Cu-Be alloy (Figure 14), the mass changes for the high humidity exposure (93% RH) were so large that a much larger scale had to be used for plotting the results than used for any other alloy. For the carbonate/bicarbonate pretreatment, the mass increased more than 100 mg for the 30 day exposure at 93% RH. This was almost an order of magnitude greater than that observed for aluminum alloy 6061 and 4130 steel and almost two orders of magnitude greater than the magnitude of the mass losses observed in the other five alloys. For the NaF pretreatment, the mass increased more than 21 mg for the 93% RH exposure (the second largest mass change observed). Clearly, in the high humidity

Table 20. Score for the Average Reduction in Area for Each Agent at 150 °C [(Mean for Envir.)-(Mean for Hot Ar)]/(Alloy Std. Dev.)

Environment	Nit 40	Al 6061	In 625	304 SS	CDA 172	13-8 Steel	AM355 SS	AISI 4130	Agent Avg.
HCFC-22	0.01	0.93	1.16	0.02	3.53	0.29	0.06	0.06	0.76
HCFC-124	0.18	2.87	1.17	0.72	2.88	0.53	0.37	0.40	1.14
FC-31-10	0.63	1.02	1.63	0.44	3.22	0.14	1.04	0.62	1.09
HFC-227	0.13	1.44	0.16	0.37	4.98	0.24	0.21	0.51	1.00
HFC-125	0.50	1.30	0.67	0.16	3.91	0.35	0.23	0.32	0.93
FC-116	0.18	0.52	0.05	0.77	4.10	0.45	0.31	0.32	0.84
HFC-134a	0.45	1.46	0.13	0.22	1.14	0.01	0.58	0.23	0.53
HFC-236	0.07	0.70	1.16	0.91	1.70	0.07	0.24	0.32	0.65
FC-C318	0.11	0.63	0.26	0.15	2.76	0.23	0.75	0.24	0.64
FC-218	2.99	0.03	0.04	0.56	1.24	0.01	0.87	0.64	0.80
HFC-32/125	0.11	0.60	0.75	0.88	3.26	0.42	0.27	0.13	0.80
NaHCO3	0.37	3.16	0.32	2.17	1.97	0.24	1.07	1.26	1.32
Alloy Avg.	0.48	1.22	0.62	0.61	2.89	0.25	0.50	0.42	

environment water vapor was absorbed onto the surface to form insoluble corrosion products at a much higher rate than at the lower humidities. Also, it appears that the addition of NaOH to the thin surface electrolyte film resulted in altering the surface films in a manner that prevented this process.

A mass increase indicates the formation of insoluble corrosion products. These corrosion products could be a protective surface film or it could be a non-protective scale. For a continuous protective film, the corrosion rate will decrease as the film grows thicker and, at least theoretically, the corrosion rate for this situation will exponentially approach zero. However, films can become non-protecting if they crack or spall as they grow allowing the environment access to bare metal through the fissures in the surface film. A non-protective scale could form as the metal corrodes to form ions in a thin electrolyte film on the surface which migrate through the electrolyte film to nucleate and grow precipitates. These precipitates grow to form relatively loose aggregate layers which do not prevent wetting of the metal by the electrolyte film nor do they prevent atmospheric gases from interacting with the thin electrolyte film, thereby allowing corrosion to continue.

The results for the aluminum alloy were a little surprising in that research has found that the hydroxide ion is the most detrimental ion with respect to the corrosion of aluminum alloys (Foley and Trazaskoma 1977). This is a direct result of the amphoteric nature of the passivating films that form on aluminum alloys and the formation of the aluminate ion (AlO_2^-). Typically, if the passive film is removed for any reason, aluminum alloys will corrode as rapidly as mass transport can provide reactants to the surface. In aqueous solutions, the passive film is stable in a pH range between 4 and 9.5. If for any reason the pH goes below or above these values the corrosion rate increases very rapidly. Apparently, adding NaOH to the artificial seawater sprayed on the surface did not increase

Table 21. Slow Strain Rate Tensile Tests at 150°C Rating for Each Alloy/Agent Combination

Environment	Nit 40	Al 6061	In 625	304 SS	CDA 172	13-8 Steel	AM355 SS	AISI 4130	Agent Avg.	Std. Dev.	Agent Rank
HCFC-22	2	1	2	1	4	2	3	2	2.13	0.99	5
HCFC-124	2	3	2	1	3	3	2	1	2.13	0.83	5
FC-31-10	2	2	2	1	4	1	3	1	2.00	1.07	3
HFC-227	2	3	1	1	5	1	3	1	2.13	1.46	5
HFC-125	1	2	1	1	4	1	4	1	1.88	1.36	2
FC-116	1	2	3	1	5	1	4	2	2.38	1.51	10
HFC-134a	2	2	3	1	2	2	3	2	2.13	0.64	5
HFC-236	2	2	2	1	2	1	3	1	1.75	0.71	1
FC-C318	1	4	1	5	3	3	2	3	2.75	1.39	11
FC-218	3	1	2	1	2	1	3	3	2.00	0.93	3
HFC-32/125	1	2	2	2	4	2	4	1	2.25	1.16	9
NaHCO3	1	4	2	3	2	6	2	2	2.75	1.58	10
Alloy Avg.	1.67	2.33	1.92	1.58	3.33	2.00	3.00	1.67			
Std. Dev.	0.65	0.98	0.67	1.24	1.15	1.48	0.74	0.78			
Alloy Rank	2	6	4	1	8	5	7	2			

Rating	Freq	Interpretation
1	31	No evidence of environment influence on deformation and fracture in this test.
2	34	Slight indication of possible environmental influence
3	18	Some evidence
4	9	Strong evidence
5	3	Nature of interaction should be evaluated.
6	1	Nature of interaction should be evaluated.
7	0	Nature of interaction should be evaluated.
8	0	Nature of interaction should be evaluated.
9	0	Nature of interaction should be evaluated.
10	0	Nature of interaction should be evaluated.

the pH of the surface electrolyte enough to destabilize the passive film. Also, it appears that increasing the humidity promoted mixing of this electrolyte film keeping the pH below critical levels and preventing the small pits which were observed at lower humidities. However, the quantity of NaOH produced by the application of a fire suppressant may exceed that applied in this experiment and pitting under droplets or particles similar to that observed in these experiments, or much worse, could occur. As a result, even though the samples treated with NaOH did not exhibit significant attack we believe that it is very risky to use a fire suppressant that produces NaOH during combustion around aluminum alloys.

The other two alloys which showed mass increases, AISI 4130 and CDA-172, are not used as commonly on aircraft as aluminum alloys. Both of these alloys showed a significant increase in the

Table 22. Summary Table of Mass Change Exposure Test Results, Crevice Corrosion Visual Examination Results and Slow Strain Rate Tensile Test Results

Environment	Expt.	Nit 40	Al 6061	In 625	304 SS	CDA 172	13-8 Steel	AM355 SS	AISI 4130	Agent Avg.
HCFC-22	Exp.	3	4	3	3	5	2	3	5	3.50
	Crevice	2	2	2	3	4	3	3	5	3.14
	SSR	2	1	2	1	4	2	3	2	2.13
HCFC-124	Exp.	3	3	3	2	4	3	3	3	3.00
	Crevice	2	2	1	2	3	3	3	5	2.63
	SSR	2	3	2	1	3	3	2	1	2.13
FC-31-10	Exp.	3	4	2	4	5	4	3	4	3.63
	Crevice	1	1	2	2	2	2	2	3	1.88
	SSR	2	2	2	1	4	1	3	1	2.00
HFC-227	Exp.	1	3	2	3	5	3	1	3	2.63
	Crevice	2	2	2	3	3	3	3	4	2.75
	SSR	2	3	1	1	5	1	3	1	2.13
HFC-125	Exp.	2	3	2	3	4	3	2	4	2.88
	Crevice	2	2	2	2	3	2	3	2	2.25
	SSR	1	2	1	1	4	1	4	1	1.88
FC-116	Exp.	1	3	2	3	4	3	3	4	2.88
	Crevice	2	2	1	2	2	3	2	3	2.13
	SSR	1	2	3	1	5	1	4	2	2.38
HFC-134a	Exp.	2	3	3	3	3	3	2	3	2.75
	Crevice	1	1	1	2	2	3	4	2	2.00
	SSR	2	2	3	1	2	2	3	2	2.13
HFC-236	Exp.	2	5	2	3	4	3	1	3	2.88
	Crevice	2	2	1	1	2	2	2	2	1.75
	SSR	2	2	2	1	2	1	3	1	1.75
FC-C318	Exp.	1	4	2	3	4	3	1	3	2.63
	Crevice	2	3	2	2	2	2	2	4	2.38
	SSR	1	4	1	5	3	3	2	3	2.75
FC-218	Exp.	3	4	2	3	4	3	3	4	3.25
	Crevice	3	4	2	2	2	2	2	4	2.63
	SSR	3	1	2	1	2	1	3	3	2.00
HFC 32/125	Exp.	3	4	3	3	5	4	3	3	3.50
	Crevice	3	2	1	2	2	2	3	4	2.38
	SSR	1	2	2	2	4	2	4	1	2.25
NaHCO3	Exp.	4	4	3	3	5	4	3	4	3.75
	Crevice	2	3	2	2	4	4	4	4	3.13
	SSR	1	4	2	3	2	6	2	2	2.75
Alloy Avg.	Exp.	2.33	3.67	2.42	3.00	4.33	3.17	2.33	3.58	
	Crevice	2.00	2.17	1.58	2.08	2.58	2.58	2.75	3.50	
	SSR	1.67	2.33	1.92	1.58	3.33	2.00	3.00	1.67	

Rating	Freq	Interpretation
1	47	No evidence of environmental attack
2	100	Some evidence of attack.
3	86	Evidence of superficial attack.
4	42	Superficial attack (more study may be required)
5	12	Attack could be a problem.
6	1	Attack needs to be considered.
7	0	Attack can be managed.
8	0	Rapid attack.
9	0	Very rapid attack.
10	0	Extremely rapid attack.

Table 23. Average Rating for Mass Change Exposure Tests, Crevice Visual Examination, and Slow Strain Rate Tensile Test

Environment	Nit 40	Al 6061	In 625	304 SS	CDA 172	13-8 Steel	AM355 SS	AISI 4130	Agent Avg.	Std. Dev.	Agent Rank
HCFC-22	2.33	2.33	2.33	2.33	4.33	2.33	3.00	4.00	2.88	0.83	11
HCFC-124	2.33	2.67	2.00	1.67	3.33	3.00	2.67	3.00	2.58	0.56	8
FC-31-10	2.33	2.33	2.00	2.33	3.67	2.33	2.67	2.67	2.50	0.53	5
HFC-227	1.67	2.67	1.67	2.33	4.33	2.33	2.33	2.67	2.50	0.84	5
HFC-125	1.67	2.33	1.67	2.00	3.67	2.00	3.00	2.33	2.33	0.69	3
FC-116	1.33	2.33	2.00	2.00	3.67	2.33	3.00	3.00	2.46	0.73	4
HFC-134a	1.67	2.00	2.33	2.00	2.33	2.67	3.00	2.33	2.29	0.42	2
HFC-236	2.00	3.00	1.67	1.67	2.67	2.00	2.00	2.00	2.13	0.47	1
FC-C318	1.33	3.67	1.67	3.33	3.00	2.67	1.67	3.33	2.58	0.90	7
FC-218	3.00	3.00	2.00	2.00	2.67	2.00	2.67	3.67	2.63	0.60	9
HFC-32/125	2.33	2.67	2.00	2.33	3.67	2.67	3.33	2.67	2.71	0.55	10
NaHCO3	2.33	3.67	2.33	2.67	3.67	4.67	3.00	3.33	3.21	0.80	12
Alloy Avg.	2.00	2.72	1.97	2.22	3.42	2.58	2.69	2.92			
Std. Dev.	0.49	0.53	0.26	0.46	0.64	0.73	0.48	0.59			
Alloy Rank	2	6	1	3	8	4	5	7			

atmospheric corrosion rate as a result of a pretreatment with NaF. As a result, cleaning the surfaces of these alloys after exposure to fire suppressant combustion products is a very good practice and substitution of another alloy which is not attack to this extent should be considered in locations where this type of exposure is expected.

7.3.3 Results of Electrochemical Measurements. The objective of these experiments was 1) to determine whether or not electrochemical measurements could be made in low conductivity electrolytes at elevated temperatures and pressures and 2) to define the lower conductivity limit for these types of measurements. As a result, a special cell was designed and constructed for this type of measurement, Figure 6. Then, experiments were conducted in an electrolyte with conductivities near and below that used by previous investigators (Halsal, 1992, deSouza, 1987). Figure 15 shows a typical impedance scan from 1 mHz to 65 kHz for 304 stainless steel in a low conductivity electrolyte (ethyl alcohol). This figure includes a Bode amplitude and phase angle plot (Figure 15(a)) and a Nyquist plot (Figure 15(b)). The resistance of the solution between the two parallel faces on the two identical samples can be determined from the Nyquist plot as the high frequency real axis (Z') intercept. By repeating these measurements at different electrode separations, a plot of the solution resistance as a function of electrode separation can be developed, Figure 16. The line in this figure is a linear regression fit through all of the resistance values determined at each separation setting. A

Table 24. Maximum (Worst) Rating for Mass Change Exposure Tests, Crevice Visual Examination, and Slow Strain Rate Tensile Test

Environment	Nit 40	Al 6061	In 625	304 SS	CDA 172	13-8 Steel	AM 355	AISI 4130	Agent Avg.	Std. Dev.	Agent Rank
HCFC-22	3	4	3	3	5	3	3	5	3.63	0.92	9
HCFC-124	3	3	3	2	4	3	3	5	3.25	0.89	5
FC-31-10	3	4	2	4	5	4	3	4	3.63	0.92	9
HFC-227	2	3	2	3	5	3	3	4	3.13	0.99	2
HFC-125	2	3	2	3	4	3	4	4	3.13	0.83	2
FC-116	2	3	3	3	5	3	4	4	3.38	0.92	8
HFC-134a	2	3	3	3	3	3	4	3	3.00	0.53	1
HFC-236	2	5	2	3	4	3	3	3	3.13	0.99	2
FC-C318	2	4	2	5	4	3	2	4	3.25	1.16	5
FC-218	3	4	2	3	4	3	3	4	3.25	0.71	5
HFC-32/125	3	4	3	3	5	4	4	4	3.75	0.71	11
NaHCO3	4	4	3	3	5	6	4	4	4.13	0.99	12
Alloy Avg.	2.58	3.67	2.50	3.17	4.42	3.42	3.33	4.00			
Std. Dev.	0.67	0.65	0.52	0.72	0.67	0.90	0.65	0.60			
Alloy Rank	2	6	1	3	8	5	4	7			

correlation coefficient of 0.978, indicating a good fit, was determined for this line. As seen from the figure, the data follow a linear relationship between the electrode separation and the resistance. Since

$$R = \rho\ (d/A), \tag{6}$$

where R is resistance, ρ is resistivity, d is the electrode separation and A is the electrode surface area. If the cell is constructed properly, the instrumentation is stable, and the experimental technique is applied properly, then one should get a linear relationship between the resistance of the electrolyte and the electrode separation as shown in this figure. However, the corrosion rate must be determined by subtracting the solution resistance, R_s, the high frequency real axis intercept in a Nyquist plot, from the cell resistance ($R_s + R_{ct}$) which is the low frequency real axis intercept in the Nyquist plot. By examining Figure 16, it can be seen the line in the Nyquist plot has not started approaching the real axis even for the lowest frequency (0.001 Hz). Since the corrosion rate is inversely proportional to the charge transfer resistance, very low frequencies will be required for these measurements even with estimating the real axis intercept from the curvature of the Nyquist plot. In addition, one can calculate the resistivity of the ethyl alcohol electrolyte from the experimental results. It is equal to

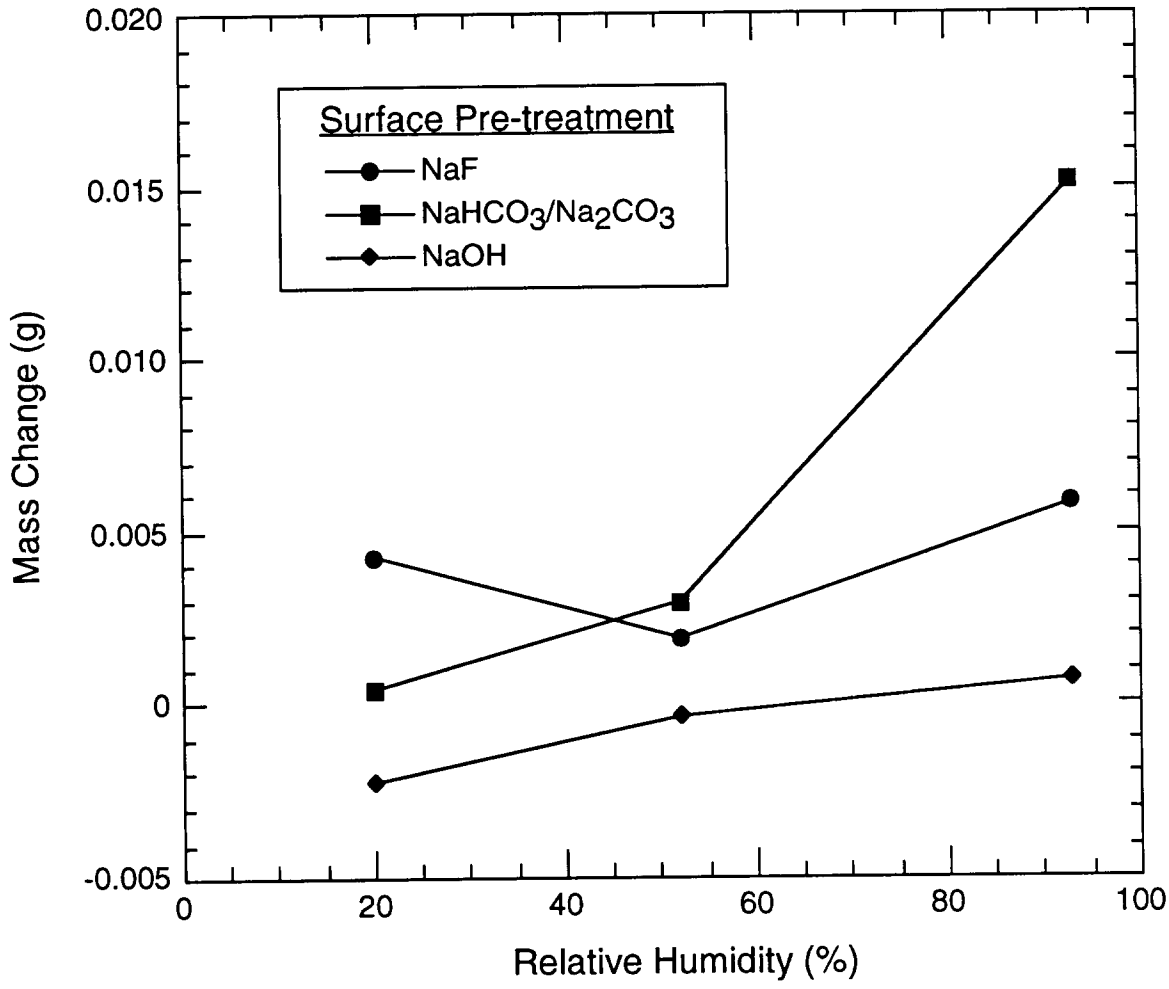

Figure 7. Mass change during atmospheric exposures at different relative humidities for aluminum alloy 6061-T6 after surface pretreatment with artificial seawater and either NaF, $NaHCO_3/Na_2CO_3$, or NaOH.

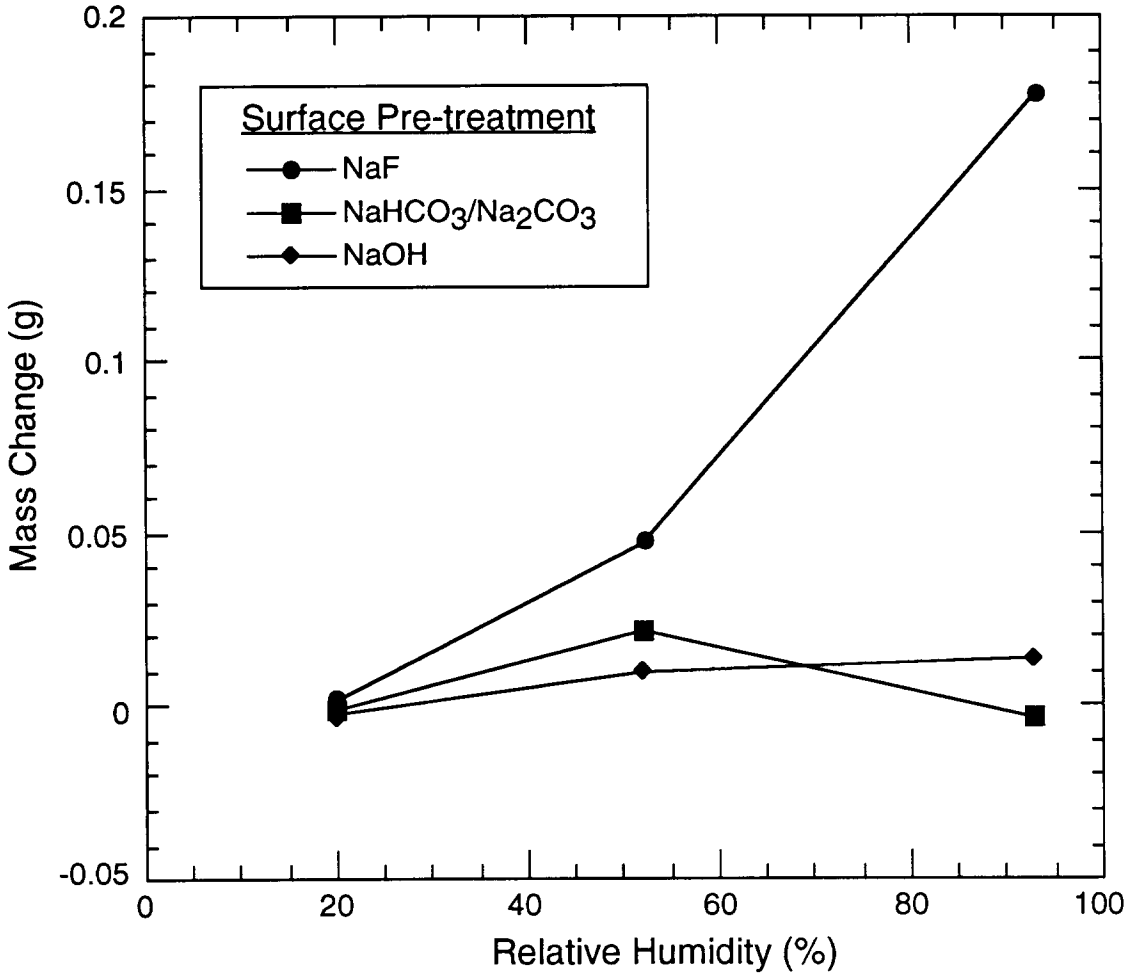

Figure 8. Mass change during atmospheric exposures at different relative humidities for AISI 4130 steel after surface pretreatment with artificial seawater and either NaF, $NaHCO_3/Na_2CO_3$, or NaOH.

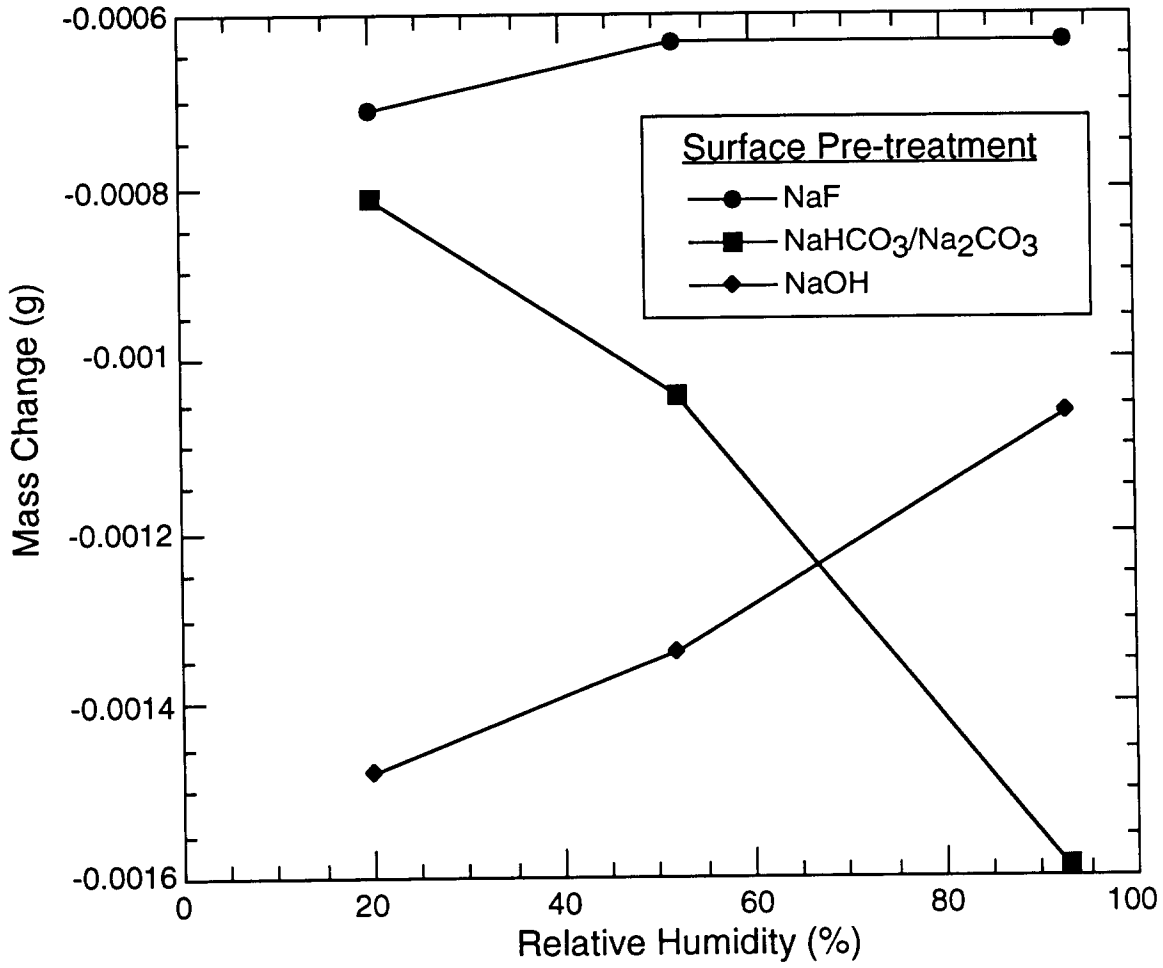

Figure 9. Mass change during atmospheric exposures at different relative humidities for 13-8 Mo steel after surface pretreatment with artificial seawater and either NaF, $NaHCO_3/Na_2CO_3$, or NaOH.

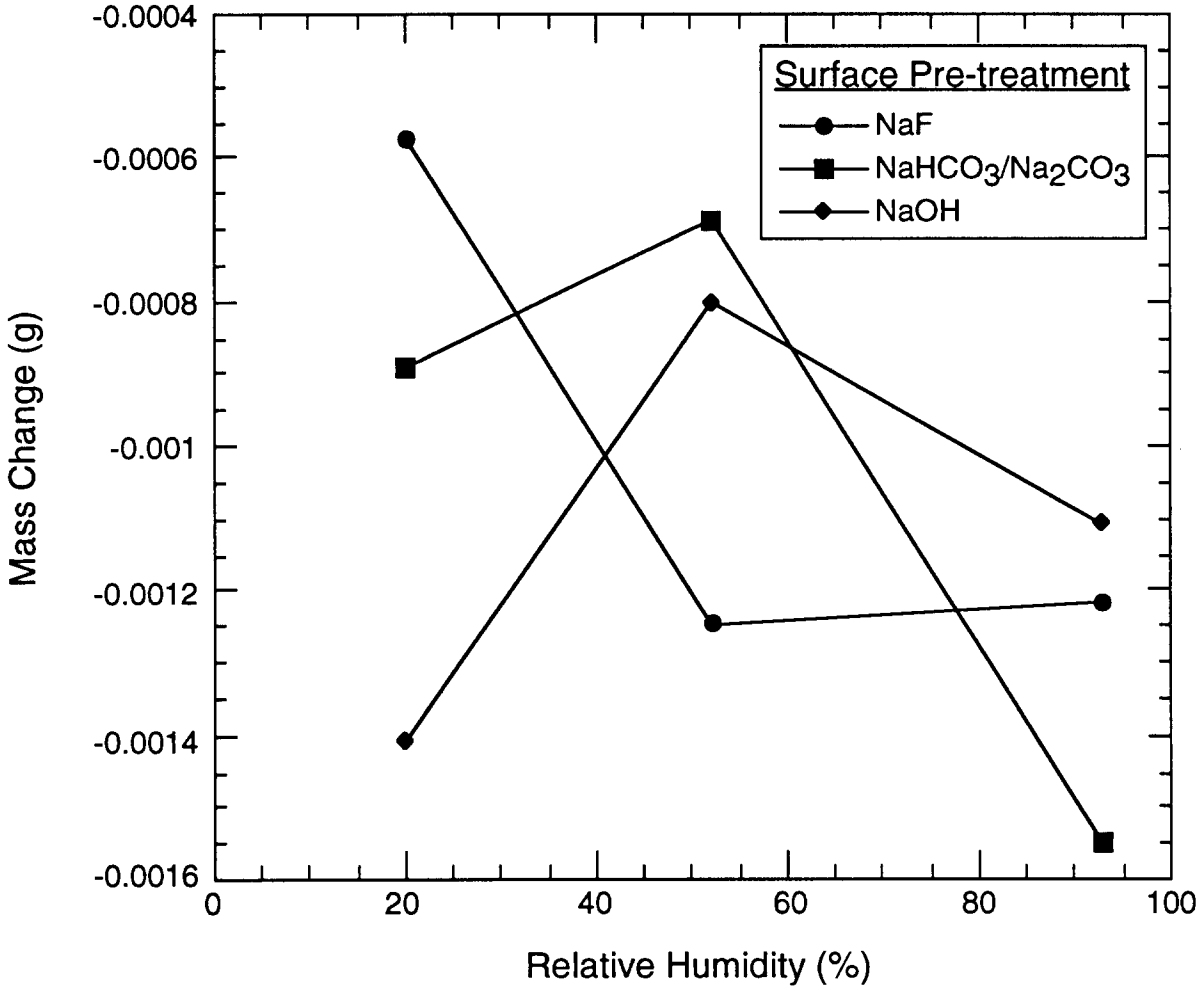

Figure 10. Mass change during atmospheric exposures at different relative humidities for AM 355 alloy after surface pretreatment with artificial seawater and either NaF, $NaHCO_3/Na_2CO_3$, or NaOH.

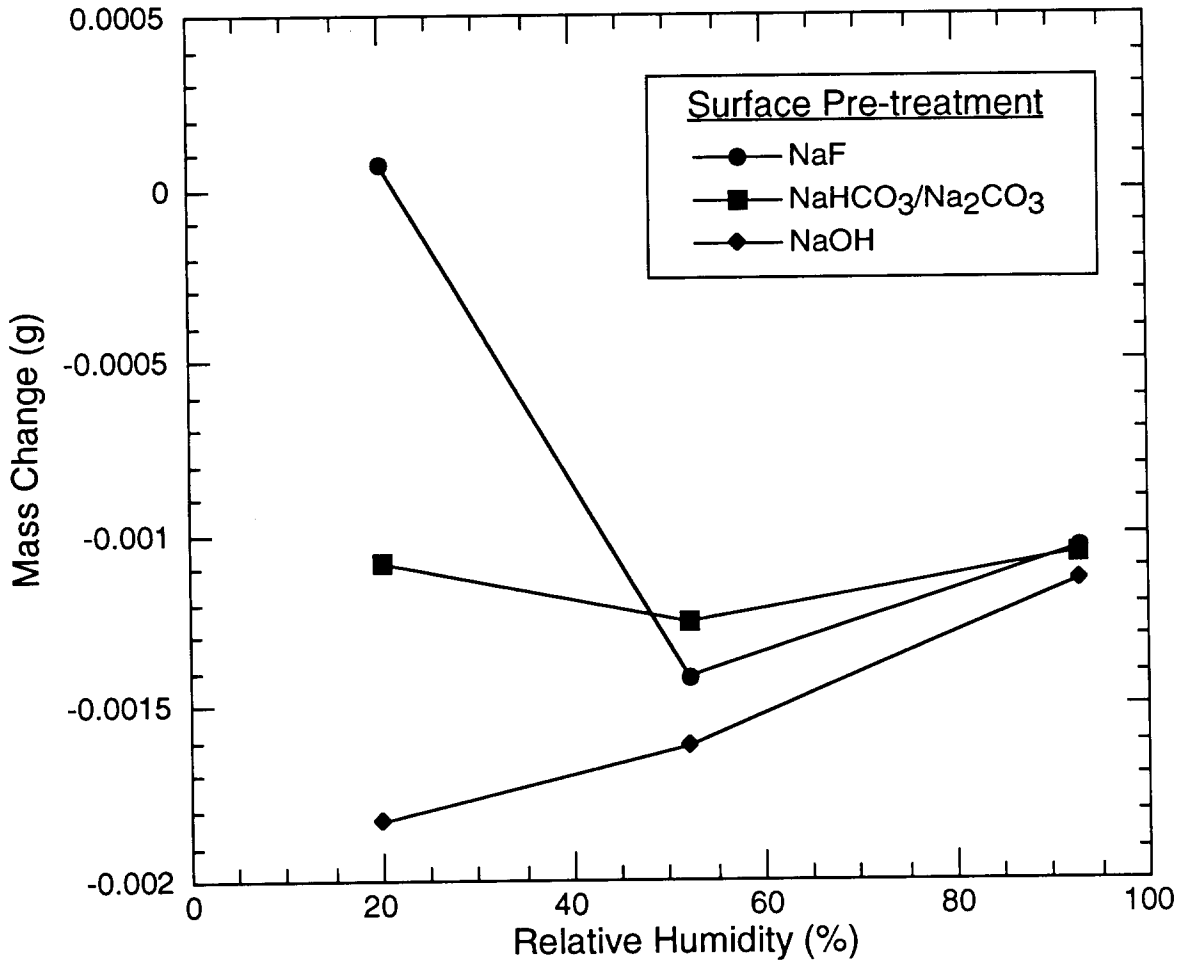

Figure 11. Mass change during atmospheric exposures at different relative humidities for 304 stainless steel after surface pretreatment with artificial seawater and either NaF, $NaHCO_3/Na_2CO_3$, or NaOH.

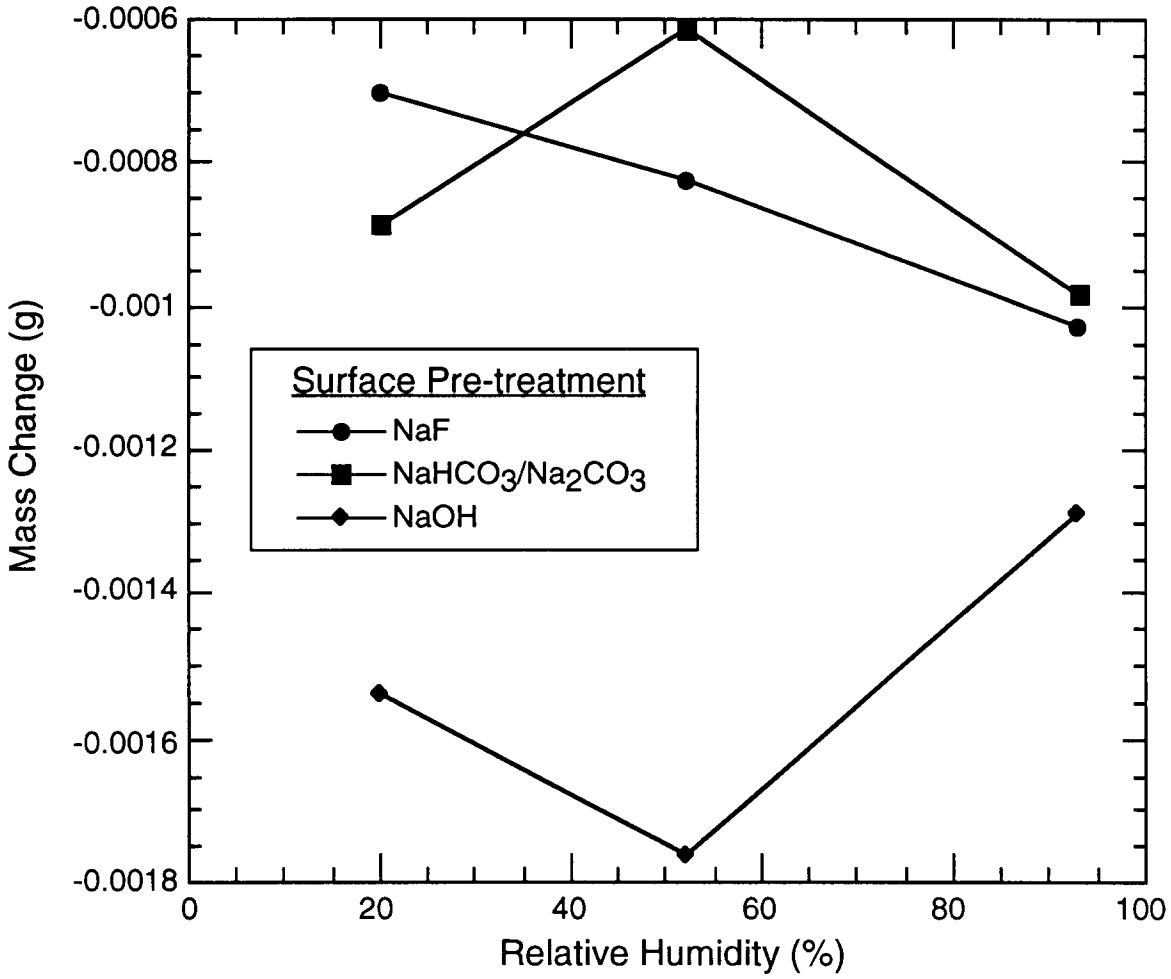

Figure 12. Mass change during atmospheric exposures at different relative humidities for Nitronic 40 alloy after surface pretreatment with artificial seawater and either NaF, $NaHCO_3/Na_2CO_3$, or NaOH.

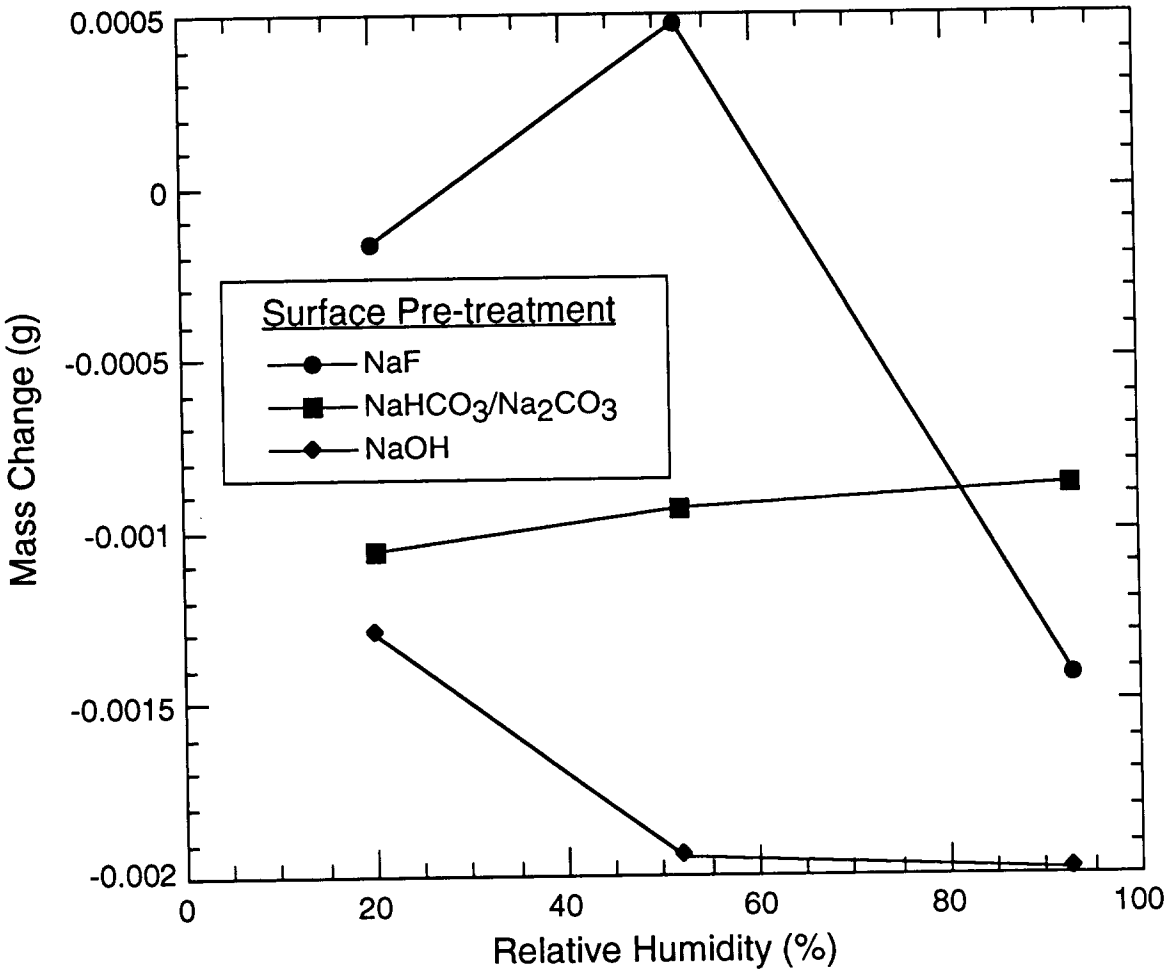

Figure 13. Mass change during atmospheric exposures at different relative humidities for Inconel 625 after surface pretreatment with artificial seawater and either NaF, $NaHCO_3/Na_2CO_3$, or NaOH.

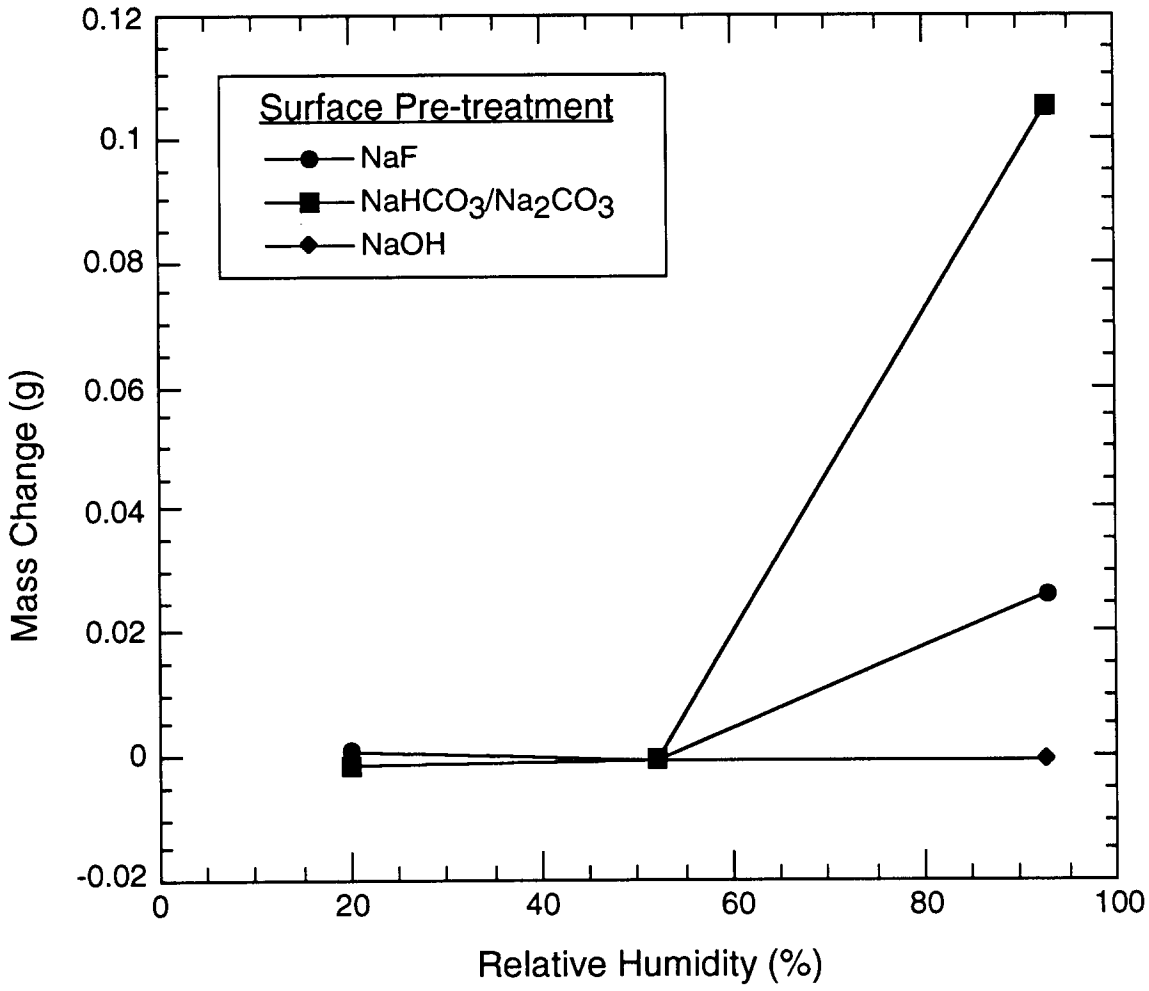

Figure 14. Mass change during atmospheric exposures at different relative humidities for the CDA 172 alloy after surface pretreatment with artificial.

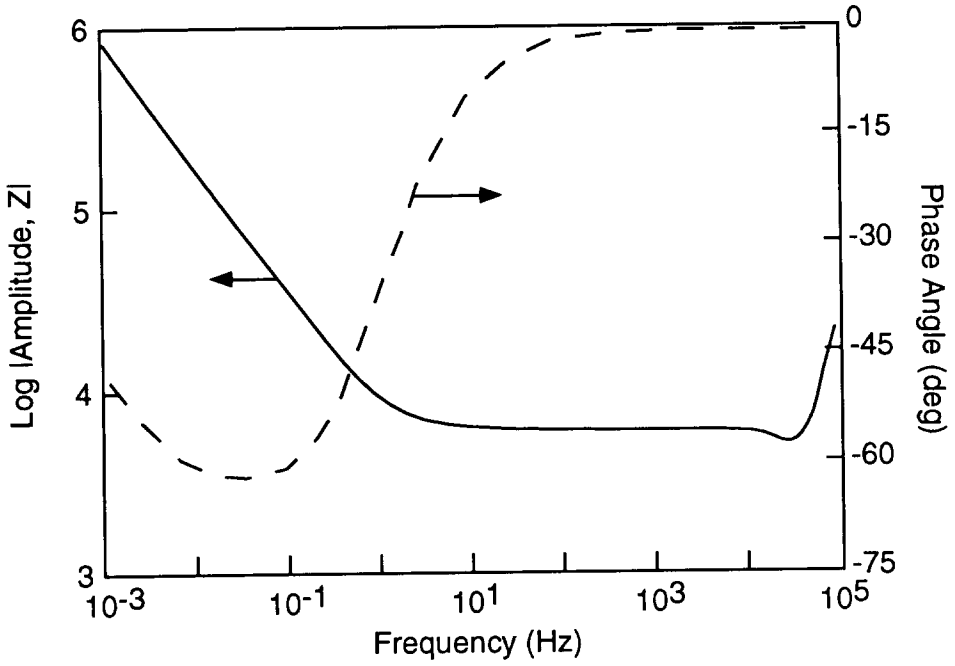

(a) Bode Amplitude and Phase Angle Plot

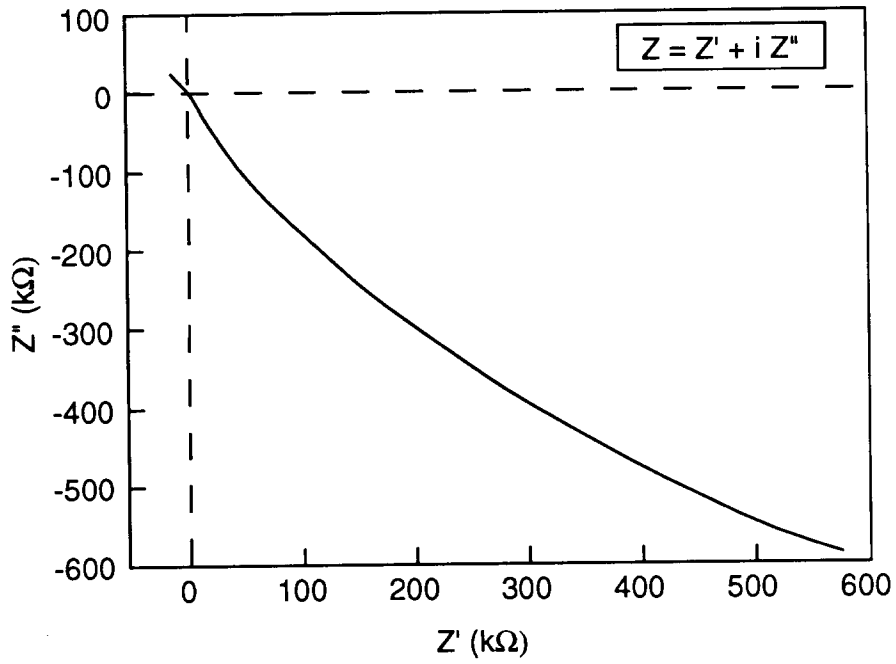

(b) Nyquist Plot

Figure 15. Bode and Nyquist plots of the impedance of 304 stainless steel in high purity ethanol.

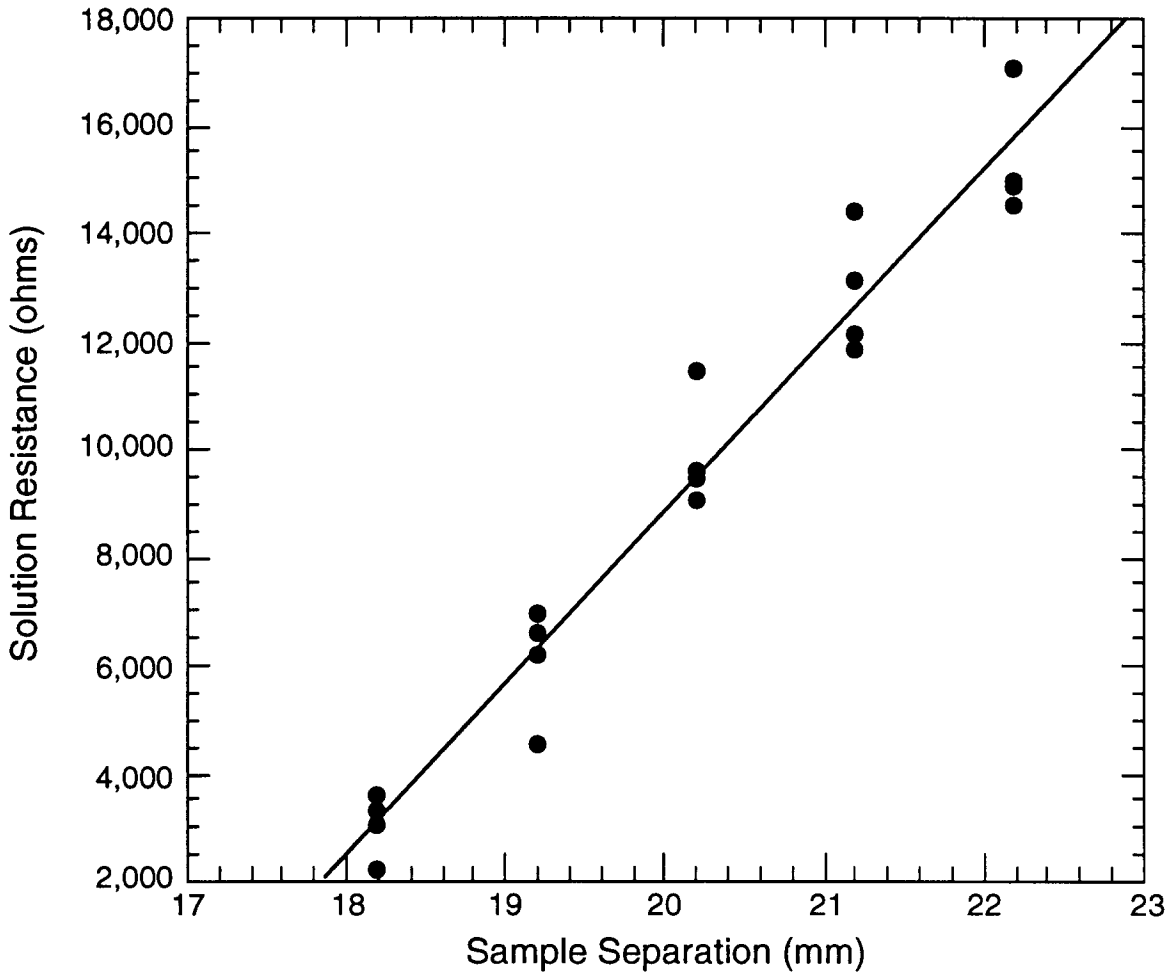

Figure 16. Solution resistance determined from two electrode impedance measurements for different electrode separations.

the slope of the curve in Figure 16 times the electrode area. Since A = 1,140 mm^2 and the slope in Figure 16 is 31,820 ohm/mm, the resistivity of the electrolyte is 3.63 x 10^7 ohm·m. This resistivity is still several orders of magnitude lower than the fire suppressants. Lowering the resistivity of the electrolyte will also make the required testing frequency range lower. As a result, other techniques for making these measurements are being explored.

7.4 Conclusions

The primary objective of this investigation was to determine if there were any of the candidates that should be eliminated from consideration because they were unacceptably corrosive to metals. This study did not identify any agent for which it would not be possible to identify a suitable alloy for the fabrication of aircraft storage and distributions systems. However, while no serious concerns were observed for all of the alloys in any of the agents, several agents consistently performed poorer than the others or yielded results that indicate further testing is warranted before they should be placed into service. Similarly, the post-deployment corrosion test results did not indicate any serious problems with any of the agents. However, the use of an agent which produces deposits of mixtures of bicarbonate, carbonate and sodium hydroxide may cause corrosion problems especially with aluminum alloys. A review of the literature on the corrosion of aluminum alloys indicates the hydroxide ion is very aggressive to these metals and very high corrosion rates can result if the pH of a surface film becomes too high. As a result, sodium bicarbonate is not considered a desirable candidate from a corrosion prevention point of view.

The secondary objective was to identify alloys that were suitable for use in each of the agents. Nitronic 40, AM 355, and 304 stainless steel consistently performed better than the other alloys in the agents, but examination of the behavior in the specific agent should be consulted before making decisions. For example, the slow strain rate tensile tests on 304 stainless steel indicated that there may be a potential environmentally induced cracking problem with this material in FC-C318, but additional testing would be required before this can be concluded.

The third objective was to develop a rapid electrochemical technique for the assessment of the corrosivity of fire suppressant agents. The technique examined enables the measurement of corrosion rates in media of much lower electrical conductivity, higher temperatures and pressures than normally examined, but very low testing frequencies and long testing times will be required for these low corrosion rate and very low conductivities. As a result, other techniques for making these measurements are being explored.

7.5 References

ASTM, Standard Guide for Applying Statistics to Analysis of Corrosion Data, *Annual Book of ASTM Standards Section 3, Metals Test Methods and Analytical Procedures*, Phil., PA, ASTM, 1993.

ASTM, Standard Practice for Laboratory Immersion Corrosion Testing of Metals, *Annual Book of ASTM Standards Section 3, Metals Test Methods and Analytical Procedures*, Phil., PA, 1993.

Bailey, J. C., Porter, F. C., and Pearson, A. W., Aluminum and Aluminum Alloys, *Corrosion*. Chapter 4.1, 4:3-4:33, Newnes - Butterworths, 1976.

Baumert, B. A., *A Study of the Corrosion Behavior of Aluminum Alloys*, Univ. of Notre Dame, Notre Dame, IN, 1986.

Bevington, P. R., *Data Reduction and Error Analysis for the Physical Sciences*, McGraw-Hill, New York, 1969.

Boyer, H. E., and Gall, T. L., *Metals Handbook— Desk Edition*, Metals Park, OH, ASM International, 1985.

Brett, C. M. A., "On the Electrochemical Behaviour of Aluminium in Acidic Chloride Solution," *Corrosion Science* 33, No. 2, 203-210, 1992.

Cabot, P. L., Centellas, F. A., Garrido, J. A., Perez, E., and Vidal, H., "Electrochemical Study of Aluminum Corrosion in Acid Chloride Solutions," *Electrochim. Acta* 36, 1, 179-187, 1991.

Davies, D. E., and Prigmore, R. M., "The Effect of Sodium Fluoride on the Localized Corrosion of Aluminum in Distilled Water and 50% Ethanediol Solution," *International Congress on Metallic Corrosion*, Toronto, Canada, National Research Council of Canads, 1984.

deSouza, J. P., Mattos, O. R., Sather, L., and Takenouti, H.,"Impedance Measurements of Corroding Mild Steel in an Automotive Fuel Ethanol With and Without Inhibitor in a Two and Three Electrode Cell." *Corro. Sci.* 27, 1351-1364, 1987.

Fink, F. W., and Boyd, W. K., *The Corrosion of Metals in Marine Environments*, Columbus, Bayer and Company Inc., Columbus, OH, 1970.

Flarsheim, W. M., Tsou, Y. M., Trachtenberg, I., Johnston, K. P., and Bard, A. J., "Electrochemistry in Near-Critical and Supercritical Fluids, 3, Studies of Br-, I-, and Hydroquionone in Aqueous Solutions", *J. Phys. Chem.*, 90, 3857-3862, 1986.

Foley, R. T., and Trazaskoma, P. P., "The Chemical Nature of the Anion Dependency of the Corrosion of Aluminum Alloy 7075-T6," *Corro.*, 33, 12, 435, 1977.

Halsall, R., *Corrosion of Metals in Ethanol and Methanol Containing Fuels*, General Motors, Warren, MI, 1992.

McDonald, A. C., Fan, F.-R. F., and Bard, A. J., "Electrochemistry in Near-Critical and Supercritical Fluids, Water, Experimental Techniques and the Copper (II) System," *J. Phys. Chem.* 90, 2, 196-202, 1986.

Mendenhall, W., and Sincich, T., *Statistics for Engineering and the Sciences*, San Francisco, Dellen Publ. Co., 1992.

Pourbaix, M., *Atlas of Electrochemical Equilibria in Aqueous Solutions. Houston, TX, National Association of Corrosion Engineers*, 1974.

Ricker, R. E., and Duquette, D. J., *Potentiodynamic Polarization Studies of an Al-Mg-Li Alloy*, Aluminum Lithium Alloys II, Warrendale, PA, The Metallurgy Society of AIME, 581-596, 1984.

Romans, H. B., and H. L. C., Jr., "Atmospheric Stress Corrosion Testing of Aluminum Alloys," *Metal Corrosion in the Atmosphere*, Boston, MA, ASTM, 1967.

Scully, J. R., Frankenthal, R. P., Hanson, K. J., Siconolfi, D. J., and Sinclair, J. D., "Localized Corrosion of Sputtered Aluminum and Al-0.5% Cu Alloy Thin Films in Aqueous HF Solution: 1 Corrosion Phenomena," *J. Electrochem. Soc.*, 137, 5, 1365-1372, 1990a.

Scully, J. R., Frankenthal, R. P., Hanson, K. J., Siconolfi, D. J., and Sinclair, J. D., "Localized Corrosion of Sputtered Aluminum and Al-0.5% Cu Aloy Thin Films in Aqueous HF Solution: II. Inhibition by CO_2," *J. Electrochem. Soc.*, 137, 1373-1377, 1990b.

Scully, J. R., Peebles, A. D., Romig, A. D., Frear, D. R., and Hills, C. R., "Metallurgical Factors Influencing the Corrosion of Aluminum, Al-Cu, and Al-Si Alloy Thin Films in Dilute Hydrofluoric Solution," *Metallurgical Transactions A* 23A, 2641-2655, September 1992.

Smith, W. F., *Structure and Properties of Engineering Alloys*, McGraw-Hill Book Company, New York, 1981.

Stoudt, M. R., Vasudévan, A. K., and Ricker, R. E., "Examination of the Influence of Lithium on the Repassivation Rate of Aluminum Alloys," *Corrosion Testing of Aluminum Alloys*, San Francisco, CA, ASTM, Phila., PA., 1990.

Walpole, R. E., and Myers, R. H., *Probability and Statistics of Engineers and Scientists*, The Macmillan Co., New York, 1972.

Wheeler, K. R., A. B. J. Jr., and May, R. P., "Aluminum Alloy Performance in Industrial Air-Cooled Applications," *Atmospheric Corrosion of Metals*, Denver, CO, ASTM, 1980A.

Zotikov, V. S., Bakhmutova, G. B., Bocharova, N. A., and Semenyuk, E. Y., "Corrosion of Al and its Alloys in Hydrofluoric Acid," *Prot. Met.*, 10, 2, 154-156, 1974.

Appendix A. Corrosion Rate Exposure Test Results

Alloy	Sample No.	Test Envir.	Average Initial Wt., grams	Average grams	Δ Wt.	Average Wt. Loss	Standard Deviation
NIT40	01	HCFC-22	14.12380	14.12393	0.00013		
NIT40	02	HCFC-22	14.31539	14.31552	0.00013	-0.00018	0.00008
NIT40	03	HCFC-22	13.78000	13.78027	0.00027		
NIT40	04	HCFC-124	14.30209	14.30217	0.00008		
NIT40	05	HCFC-124	14.11364	14.11370	0.00006	-0.00009	0.00005
NIT40	06	HCFC-124	14.14462	14.14476	0.00014		
NIT40	07	FC-31-10	14.01056	14.01079	0.00022		
NIT40	08	FC-31-10	14.07978	14.08000	0.00022	-0.00025	0.00004
NIT40	09	FC-31-10	14.03391	14.03421	0.00029		
NIT40	10	HFC-227	14.26208	14.26211	0.00003		
NIT40	11	HFC-227	14.21813	14.21816	0.00003	-0.00001	0.00003
NIT40	12	HFC-227	14.15156	14.15153	-0.00003		
NIT40	13	HFC-125	14.29082	14.29093	0.00012		
NIT40	14	HFC-125	14.21129	14.21117	-0.00012	0.00001	0.00012
NIT40	15	HFC-125	13.91204	13.91201	-0.00003		
NIT40	16	FC-116	14.09377	14.09379	0.00002		
NIT40	17	FC-116	13.88219	13.88232	0.00012	-0.00001	0.00012
NIT40	18	FC-116	14.06229	14.06216	-0.00012		
NIT40	19	HFC-134a	13.94796	13.94795	-0.00001		
NIT40	20	HFC-134a	14.24534	14.24537	0.00003	-0.00001	0.00002
NIT40	21	HFC-134a	14.21014	14.21016	0.00002		
NIT40	22	HFC-236	14.12528	14.12532	0.00004		
NIT40	23	HFC-236	14.11809	14.11812	0.00004	-0.00002	0.00002
NIT40	24	HFC-236	14.26927	14.26926	0.00000		
NIT40	25	FC-C318	14.35759	14.35764	0.00005		
NIT40	26	FC-C318	14.33708	14.33707	-0.00001	-0.00001	0.00004
NIT40	27	FC-C318	14.18774	14.18772	-0.00002		
NIT40	28	FC-218	14.30586	14.30608	0.00022		
NIT40	29	FC-218	13.95517	13.95535	0.00018	-0.00015	0.00008
NIT40	30	FC-218	14.27204	14.27210	0.00006		
NIT40	1a	HFC-32/125	14.85542	14.85569	0.00027		
NIT40	2a	HFC-32/125	14.79800	14.79830	0.00030	-0.00030	0.00003
NIT40	3a	HFC-32/125	14.79587	14.79621	0.00033		
NIT40	4a	NaHCO3	14.82673	14.82690	0.00017		
NIT40	5a	NaHCO3	14.79937	14.79965	0.00028	-0.00040	0.00030
NIT40	6a	NaHCO3	14.80710	14.80783	0.00073		
6061-T6	01	HCFC-22	5.15897	5.15956	0.00059		
6061-T6	02	HCFC-22	5.14160	5.14202	0.00041	-0.00046	0.00011
6061-T6	03	HCFC-22	5.16151	5.16188	0.00037		
6061-T6	04	HCFC-124	5.15992	5.16021	0.00029		

Alloy	Sample No.	Test Envir.	Average Initial Wt., grams	Average grams	Δ Wt.	Average Wt. Loss	Standard Deviation
NIT40	01	HCFC-22	14.12380	14.12393	0.00013		
6061-T6	05	HCFC-124	5.15997	5.16009	0.00012	-0.00022	0.00009
6061-T6	06	HCFC-124	5.16249	5.16274	0.00025		
6061-T6	07	FC-31-10	5.15805	5.15867	0.00062		
6061-T6	08	FC-31-10	5.15762	5.15808	0.00047	-0.00053	0.00008
6061-T6	09	FC-31-10	5.15774	5.15825	0.00051		
6061-T6	10	HFC-227	5.14240	5.14254	0.00014		
6061-T6	11	HFC-227	5.15458	5.15475	0.00016	-0.00013	0.00004
6061-T6	12	HFC-227	5.16393	5.16401	0.00008		
6061-T6	13	HFC-125	5.14067	5.14096	0.00029		
6061-T6	14	HFC-125	5.14888	5.14912	0.00024	-0.00020	0.00012
6061-T6	15	HFC-125	5.16261	5.16267	0.00007		
6061-T6	16	FC-116	5.14425	5.14459	0.00034		
6061-T6	17	FC-116	5.16136	5.16155	0.00018	-0.00024	0.00009
6061-T6	18	FC-116	5.15905	5.15924	0.00020		
6061-T6	19	HFC-134a	5.15888	5.15901	0.00013		
6061-T6	20	HFC-134a	5.15054	5.15069	0.00016	-0.00013	0.00003
6061-T6	21	HFC-134a	5.13945	5.13955	0.00011		
6061-T6	22	HFC-236	5.15121	5.15562	0.00442		
6061-T6	23	HFC-236	5.14617	5.14856	0.00239	-0.00248	0.00189
6061-T6	24	HFC-236	5.15225	5.15288	0.00063		
6061-T6	25	FC-C318	5.15709	5.15884	0.00174		
6061-T6	26	FC-C318	5.15927	5.16053	0.00126	-0.00118	0.00060
6061-T6	27	FC-C318	5.14241	5.14295	0.00055		
6061-T6	01a	FC-218	5.10076	5.10108	0.00032		
6061-T6	02a	FC-218	5.11183	5.11221	0.00039	-0.00037	0.00005
6061-T6	03a	FC-218	5.11843	5.11884	0.00041		
6061-T6	10a	HFC-32/125	5.11563	5.11658	0.00095		
6061-T6	11a	HFC-32/125	5.11169	5.11215	0.00047	-0.00059	0.00032
6061-T6	12a	HFC-32/125	5.11423	5.11457	0.00034		
6061-T6	13a	NaHCO3	5.10236	5.10328	0.00092		
6061-T6	14a	NaHCO3	5.11181	5.11242	0.00061	-0.00104	0.00050
6061-T6	15a	NaHCO3	5.11315	5.11474	0.00159		
I625	01	HCFC-22	16.71024	16.70993	-0.00031		
I625	02	HCFC-22	16.73534	16.73509	-0.00025	0.00033	0.00009
I625	03	HCFC-22	16.74050	16.74008	-0.00042		
I625	04	HCFC-124	16.72578	16.72552	-0.00025		
I625	05	HCFC-124	16.71996	16.71964	-0.00032	0.00027	0.00005
I625	06	HCFC-124	16.78778	16.78755	-0.00023		
I625	07	FC-31-10	16.73050	16.73044	-0.00007		
I625	08	FC-31-10	16.71615	16.71614	-0.00001	0.00004	0.00003

Alloy	Sample No.	Test Envir.	Average Initial Wt., grams	Average grams	Δ Wt.	Average Wt. Loss	Standard Deviation
NIT40	01	HCFC-22	14.12380	14.12393	0.00013		
I625	09	FC-31-10	16.43237	16.43234	-0.00003		
I625	10	HFC-227	16.73460	16.73455	-0.00005		
I625	11	HFC-227	16.73019	16.73015	-0.00004	0.00006	0.00002
I625	12	HFC-227	16.78825	16.78818	-0.00008		
I625	13	HFC-125	16.72097	16.72095	-0.00002		
I625	14	HFC-125	16.70044	16.70050	0.00006	-0.00003	0.00004
I625	15	HFC-125	16.72375	16.72380	0.00005		
I625	16	FC-116	16.79899	16.79900	0.00002		
I625	17	FC-116	16.76286	16.76287	0.00001	-0.00003	0.00002
I625	18	FC-116	16.80056	16.80061	0.00005		
I625	19	HFC-134a	16.72989	16.72981	-0.00008		
I625	20	HFC-134a	16.40575	16.40562	-0.00013	0.00010	0.00002
I625	21	HFC-134a	16.72400	16.72390	-0.00010		
I625	22	HFC-236	16.38116	16.38111	-0.00005		
I625	23	HFC-236	16.71103	16.71099	-0.00004	0.00006	0.00003
I625	24	HFC-236	16.73446	16.73437	-0.00010		
I625	25	FC-C318	16.79867	16.79876	0.00009		
I625	26	FC-C318	16.68154	16.68152	-0.00002	-0.00002	0.00007
I625	27	FC-C318	16.73452	16.73450	-0.00002		
I625	01a	FC-218	17.04525	17.04529	0.00004		
I625	02a	FC-218	17.04924	17.04931	0.00006	-0.00005	0.00001
I625	03a	FC-218	17.03955	17.03959	0.00005		
I625	10a	HFC-32/125	17.04597	17.04613	0.00016		
I625	11a	HFC-32/125	17.02094	17.02106	0.00012	-0.00015	0.00002
I625	12a	HFC-32/125	17.03789	17.03805	0.00016		
I625	13a	NaHCO3	17.00623	17.00631	0.00008		
I625	14a	NaHCO3	16.98212	16.98218	0.00006	-0.00008	0.00002
I625	15a	NaHCO3	17.00205	17.00215	0.00010		
304	01	HCFC-22	14.50690	14.50701	0.00011		
304	02	HCFC-22	14.54831	14.54854	0.00022	-0.00017	0.00006
304	03	HCFC-22	14.54721	14.54738	0.00017		
304	04	HCFC-124	14.55392	14.55389	-0.00003		
304	05	HCFC-124	14.52197	14.52197	0.00000	0.00004	0.00004
304	06	HCFC-124	14.55766	14.55758	-0.00008		
304	07	FC-31-10	14.57636	14.57693	0.00057		
304	08	FC-31-10	14.59461	14.59524	0.00062	-0.00058	0.00004
304	09	FC-31-10	14.53066	14.53122	0.00056		
304	10	HFC-227	14.50282	14.50297	0.00015		
304	11	HFC-227	14.48668	14.48684	0.00016	-0.00014	0.00002
304	12	HFC-227	14.49441	14.49453	0.00011		

Alloy	Sample No.	Test Envir.	Average Initial Wt., grams	Average grams	Δ Wt.	Average Wt. Loss	Standard Deviation
NIT40	01	HCFC-22	14.12380	14.12393	0.00013		
304	13	HFC-125	14.53445	14.53459	0.00014		
304	14	HFC-125	14.58747	14.58759	0.00012	-0.00014	0.00001
304	15	HFC-125	14.51819	14.51834	0.00014		
304	16	FC-116	14.60180	14.60199	0.00018		
304	17	FC-116	14.58646	14.58660	0.00014	-0.00015	0.00003
304	18	FC-116	14.56847	14.56859	0.00012		
304	19	HFC-134a	14.54856	14.54863	0.00007		
304	20	HFC-134a	14.57147	14.57154	0.00007	-0.00007	0.00000
304	21	HFC-134a	14.51002	14.51008	0.00007		
304	22	HFC-236	14.50289	14.50299	0.00009		
304	23	HFC-236	14.56563	14.56573	0.00010	-0.00008	0.00003
304	24	HFC-236	14.49324	14.49329	0.00004		
304	25	FC-C318	14.55940	14.55956	0.00016		
304	26	FC-C318	14.48874	14.48892	0.00018	-0.00020	0.00005
304	27	FC-C318	14.52980	14.53006	0.00026		
304	01a	FC-218	14.70650	14.70657	0.00007		
304	02a	FC-218	14.59916	14.59922	0.00005	-0.00009	0.00005
304	03a	FC-218	14.67582	14.67597	0.00015		
304	10a	HFC-32/125	14.62390	14.62411	0.00021		
304	11a	HFC-32/125	14.72853	14.72875	0.00023	-0.00024	0.00004
304	12a	HFC-32/125	14.66874	14.66902	0.00028		
304	13a	NaHCO3	14.66832	14.66853	0.00021		
304	14a	NaHCO3	14.71106	14.71136	0.00030	-0.00026	0.00005
304	15a	NaHCO3	14.57512	14.57540	0.00028		
172	01	HCFC-22	16.08959	16.09228	0.00269		
172	02	HCFC-22	16.60931	16.61261	0.00331	-0.00306	0.00033
172	03	HCFC-22	16.35164	16.35484	0.00320		
172	04	HCFC-124	16.37510	16.37691	0.00181		
172	05	HCFC-124	16.38782	16.38919	0.00137	-0.00147	0.00029
172	06	HCFC-124	16.31289	16.31414	0.00125		
172	07	FC-31-10	16.47673	16.47927	0.00254		
172	08	FC-31-10	16.47398	16.47671	0.00273	-0.00266	0.00011
172	09	FC-31-10	16.15224	16.15496	0.00272		
172	10	HFC-227	16.42018	16.42233	0.00215		
172	11	HFC-227	16.20014	16.20199	0.00185	-0.00197	0.00016
172	12	HFC-227	16.52838	16.53030	0.00192		
172	13	HFC-125	16.57400	16.57489	0.00088		
172	14	HFC-125	16.60772	16.60860	0.00088	-0.00089	0.00002
172	15	HFC-125	16.48618	16.48709	0.00091		
172	16	FC-116	16.53656	16.53792	0.00136		

Alloy	Sample No.	Test Envir.	Average Initial Wt., grams	Average grams	Δ Wt.	Average Wt. Loss	Standard Deviation
NIT40	01	HCFC-22	14.12380	14.12393	0.00013		
172	17	FC-116	16.41082	16.41249	0.00167	-0.00151	0.00016
172	18	FC-116	16.52522	16.52671	0.00149		
172	19	HFC-134a	16.18493	16.18514	0.00021		
172	20	HFC-134a	16.48381	16.48401	0.00020	-0.00023	0.00004
172	21	HFC-134a	16.37599	16.37626	0.00027		
172	22	HFC-236	16.52102	16.52189	0.00087		
172	23	HFC-236	16.49087	16.49177	0.00089	-0.00087	0.00003
172	24	HFC-236	16.82507	16.82590	0.00084		
172	25	FC-C318	16.27482	16.27525	0.00043		
172	26	FC-C318	16.47234	16.47284	0.00050	-0.00043	0.00007
172	27	FC-C318	16.52698	16.52734	0.00036		
172	01a	FC-218	16.65123	16.65199	0.00077		
172	02a	FC-218	16.61390	16.61470	0.00080	-0.00077	0.00003
172	03a	FC-218	16.71205	16.71278	0.00074		
172	10a	HFC-32/125	16.64347	16.64594	0.00247		
172	11a	HFC-32/125	16.67785	16.67989	0.00204	-0.00226	0.00022
172	12a	HFC-32/125	16.56278	16.56506	0.00228		
172	13a	NaHCO3	16.69064	16.69282	0.00218		
172	14a	NaHCO3	16.69839	16.70081	0.00242	-0.00218	0.00024
172	15a	NaHCO3	16.60099	16.60294	0.00195		
13-8	01	HCFC-22	15.04714	15.04715	0.00001		
13-8	02	HCFC-22	15.16177	15.16169	-0.00008	0.00003	0.00004
13-8	03	HCFC-22	15.07196	15.07193	-0.00003		
13-8	04	HCFC-124	15.41550	15.41533	-0.00017		
13-8	05	HCFC-124	15.21775	15.21769	-0.00006	0.00009	0.00007
13-8	06	HCFC-124	15.01510	15.01507	-0.00003		
13-8	07	FC-31-10	15.37818	15.37857	0.00039		
13-8	08	FC-31-10	15.26949	15.26977	0.00028	-0.00036	0.00007
13-8	09	FC-31-10	15.15930	15.15971	0.00041		
13-9	10	HFC-227	15.19980	15.19988	0.00008		
13-8	11	HFC-227	15.14515	15.14527	0.00012	-0.00007	0.00006
13-8	12	HFC-227	15.36752	15.36752	0.00000		
13-8	13	HFC-125	15.32942	15.32956	0.00014		
13-8	14	HFC-125	15.26229	15.26243	0.00015	-0.00015	0.00001
13-8	15	HFC-125	15.13633	15.13649	0.00017		
13-8	16	FC-116	15.05156	15.05179	0.00022		
13-8	17	FC-116	14.98056	14.98077	0.00021	-0.00021	0.00001
13-8	18	FC-116	15.21466	15.21486	0.00020		
13-8	19	HFC-134a	15.42397	15.42412	0.00015		
13-8	20	HFC-134a	15.22669	15.22673	0.00003	-0.00009	0.00006

Alloy	Sample No.	Test Envir.	Average Initial Wt., grams	Average grams	Δ Wt.	Average Wt. Loss	Standard Deviation
NIT40	01	HCFC-22	14.12380	14.12393	0.00013		
13-8	21	HFC-134a	15.15183	15.15190	0.00008		
13-8	22	HFC-236	15.12782	15.12793	0.00012		
13-8	23	HFC-236	15.01663	15.01672	0.00009	-0.00011	0.00001
13-8	24	HFC-236	15.34009	15.34021	0.00011		
13-8	25	FC-C318	15.09380	15.09395	0.00015		
13-8	26	FC-C318	15.37339	15.37357	0.00018	-0.00017	0.00001
13-8	27	FC-C318	15.44205	15.44223	0.00017		
13-8	01a	FC-218	15.29468	15.29494	0.00026		
13-8	02a	FC-218	15.10975	15.11002	0.00027	-0.00028	0.00002
13-8	03a	FC-218	15.23719	15.23749	0.00030		
13-9	10a	HFC-32/125	15.11540	15.11581	0.00042		
13-8	11a	HFC-32/125	15.34063	15.34103	0.00041	-0.00049	0.00014
13-8	12a	HFC-32/125	15.03324	15.03389	0.00065		
13-8	13a	NaHCO3	14.85465	14.85575	0.00110		
13-8	14a	NaHCO3	15.10975	15.11041	0.00066	-0.00080	0.00026
13-8	15a	NaHCO3	15.08130	15.08194	0.00064		
355	01	HCFC-22	15.29150	15.29145	-0.00005		
355	02	HCFC-22	15.00926	15.00912	-0.00014	0.00009	0.00005
355	03	HCFC-22	15.32792	15.32785	-0.00007		
355	04	HCFC-124	15.01662	15.01629	-0.00032		
355	05	HCFC-124	15.42594	15.42581	-0.00013	0.00021	0.00010
355	06	HCFC-124	14.92252	14.92236	-0.00016		
355	07	FC-31-10	14.98140	14.98163	0.00023		
355	08	FC-31-10	15.39432	15.39458	0.00026	-0.00022	0.00005
355	09	FC-31-10	15.36341	15.36358	0.00017		
355	10	HFC-227	15.51429	15.51431	0.00002		
355	11	HFC-227	15.39858	15.39860	0.00002	-0.00001	0.00002
355	12	HFC-227	14.84048	14.84047	-0.00002		
355	13	HFC-125	14.97517	14.97520	0.00003		
355	14	HFC-125	14.75849	14.75853	0.00004	-0.00003	0.00001
355	15	HFC-125	15.34143	15.34145	0.00002		
355	16	FC-116	15.23439	15.23460	0.00021		
355	17	FC-116	14.88056	14.88069	0.00013	-0.00014	0.00006
355	18	FC-116	14.87070	14.87078	0.00008		
355	19	HFC-134a	14.89687	14.89690	0.00003		
355	20	HFC-134a	15.51394	15.51393	0.00000	0.00001	0.00005
355	21	HFC-134a	14.97787	14.97780	-0.00007		
355	22	HFC-236	15.26546	15.26536	-0.00010		
355	23	HFC-236	14.88965	14.88972	0.00007	-0.00001	0.00009
355	24	HFC-236	15.50902	15.50906	0.00005		

Alloy	Sample No.	Test Envir.	Average Initial Wt., grams	Average grams	Δ Wt.	Average Wt. Loss	Standard Deviation
NIT40	01	HCFC-22	14.12380	14.12393	0.00013		
355	25	FC-C318	14.74122	14.74128	0.00006		
355	26	FC-C318	15.22578	15.22585	0.00007	-0.00001	0.00011
355	27 *	FC-C318	14.74538	14.74526	-0.00012		
355	01a	FC-218	15.33161	15.33171	0.00010		
355	02a	FC-218	15.71182	15.71198	0.00016	-0.00015	0.00004
355	03a	FC-218	15.27753	15.27772	0.00019		
355	10a	HFC-32/125	15.39200	15.39234	0.00034		
355	11a	HFC-32/125	15.44073	15.44101	0.00027	-0.00031	0.00004
355	12a	HFC-32/125	15.36869	15.36901	0.00032		
355	13a	NaHCO3	15.52390	15.52416	0.00026		
355	14a	NaHCO3	15.52734	15.52756	0.00022	-0.00026	0.00004
355	15a	NaHCO3	15.46160	15.46190	0.00030		
4130	01	HCFC-22	15.65953	15.66151	0.00198		
4130	02	HCFC-22	15.60112	15.60544	0.00432	-0.00285	0.00128
4130	03	HCFC-22	15.62642	15.62867	0.00225		
4130	04	HCFC-124	15.64049	15.64073	0.00024		
4130	05	HCFC-124	15.67752	15.67795	0.00043	-0.00032	0.00010
4130	06	HCFC-124	15.63756	15.63785	0.00029		
4130	07	FC-31-10	15.66338	15.66454	0.00116		
4130	08	FC-31-10	15.68480	15.68603	0.00124	-0.00110	0.00017
4130	09	FC-31-10	15.71161	15.71252	0.00091		
4130	10	HFC-227	15.66745	15.66773	0.00028		
4130	11	HFC-227	15.69433	15.69459	0.00026	-0.00030	0.00005
4130	12	HFC-227	15.69102	15.69137	0.00035		
4130	13	HFC-125	15.67280	15.67345	0.00065		
4130	14	HFC-125	15.69388	15.69465	0.00077	-0.00067	0.00009
4130	15	HFC-125	15.61443	15.61503	0.00060		
4130	16	FC-116	15.67118	15.67160	0.00042		
4130	17	FC-116	15.65998	15.66037	0.00039	-0.00040	0.00001
4130	18	FC-116	15.63905	15.63945	0.00040		
4130	19	HFC-134a	15.65736	15.65765	0.00029		
4130	20	HFC-134a	15.67523	15.67539	0.00016	-0.00026	0.00009
4130	21	HFC-134a	15.68774	15.68808	0.00033		
4130	22	HFC-236	15.64327	15.64356	0.00029		
4130	23	HFC-236	15.70320	15.70357	0.00037	-0.00034	0.00004
4130	24	HFC-236	15.72882	15.72919	0.00037		
4130	25	FC-C318	15.67104	15.67137	0.00034		
4130	26	FC-C318	15.69345	15.69372	0.00027	-0.00031	0.00004
4130	27	FC-C318	15.67568	15.67600	0.00032		
4130	01a	FC-218	15.63867	15.63896	0.00029		

Alloy	Sample No.	Test Envir.	Average Initial Wt., grams	Average grams	Δ Wt.	Average Wt. Loss	Standard Deviation
NIT40	01	HCFC-22	14.12380	14.12393	0.00013		
4130	02a	FC-218	15.66631	15.66673	0.00042	-0.00038	0.00008
4130	03a	FC-218	15.57494	15.57537	0.00044		
4130	10a	HFC-32/125	15.68322	15.68357	0.00035		
4130	11a	HFC-32/125	15.72594	15.72617	0.00023	-0.01134	0.01914
4130	12a	HFC-32/125	15.65444	15.68788	0.03344		
4130	13a	NaHCO3	15.67555	15.67662	0.00107		
4130	14a	NaHCO3	15.63064	15.63150	0.00086	-0.00089	0.00017
4130	15a	NaHCO3	15.69020	15.69093	0.00074		